CORRESPONDENCE

Anti-MDA5 antibody-positive dermatomyositis with lethal progressive interstitial lung disease and advanced gastric cancer

Dermatomyositis (DM) is an autoimmune inflammatory disease often associated with internal malignancy and interstitial lung disease. The latter is found in about 50% of patients with DM and is a life-threatening complication of the disease [1]. Rapidly progressive interstitial lung disease (RP-ILD) associated with clinically amyopathic dermatomyositis (CADM) is often lethal, despite treatment by corticosteroid therapy combined with immunosuppressive drugs [2].

A number of autoantibodies can be detected in sera of patients with DM, some specific to RP-ILD. Recently, there have been reports that anti-melanoma differentiation-associated gene 5 (MDA5) antibody predicts a fatal outcome in patients with DM complicated by RP-ILD [3]. A close association has been described between the presence of anti-transcription intermediary factor 1γ (anti-TIF-1γ) antibodies and internal malignancy in DM patients [4].

We report a RP-ILD and advanced gastric cancer in a case of anti-MDA5 antibody-positive and anti-TIF-1γ antibody-negative DM. The patient, a 64-year-old Japanese woman, had suffered from photosensitivity, proximal muscle weakness and dyspnea on exertion for the past 4 weeks. Further evaluations, including electromyography, upper endoscopy and thoracoabdominal computed tomography, revealed DM complicated by interstitial lung disease, advanced gastric cancer and paraaortic lymph node swelling. The biopsy specimen from her stomach was positive for poorly-differentiated adenocarcinoma cells. Subsequently, the lung disease progressed rapidly, resulting in a drop of blood oxygenation to a level interfering with her daily activities. At this point, she was referred to our hospital.

Physical examination revealed red-to-violaceous, well demarcated plaques on the face (*figure 1A*), limbs and sacrum. Gottron's papules (*figures 1B-E*), periungual erythema, and nail-fold bleeding on the hands were found. Histopathological examination of skin biopsies from the dorsal interphalangeal joint found hyperkeratosis, atrophy and superficial dermal inflammation with overlying interfacial change (*figure 1F,G*). Laboratory investigations identified increased levels of serum lactate dehydrogenase (611 IU/L), C-reactive protein (5.38 mg/dL), ferritin (1030 ng/mL), creatine kinase (620 IU/L), aldolase (16 U/L), myoglobin (110 ng/mL), carcinoembryonic antigen (28 ng/mL), cancer antigen 19-9 (136 U/mL), KL-6 (1713 U/mL) and surfactant protein-D (105 ng/mL). The oxygen saturation level from a finger probe was 84%, despite the inhalation of oxygen at a rate of 3 L per minute by nasal canula. Arterial blood gas analysis under the same conditions showed mild hypoxia (pH 7.489; PaO_2, 76.2 Torr; $PaCO_2$, 32.3 Torr). Anti-MDA5 antibody was detected by immunoprecipitation [5] and specific enzyme-linked immunosorbent assays.

Intensive therapies, including steroid pulse (1 g/day for 3 days) and cyclosporine (200 mg/day), were administered after the diagnosis of RP-ILD as a complication. These therapies did not improve her respiratory status and the serum muscular enzyme levels decreased. Meanwhile, serum ferritin levels were markedly elevated. At 31 days after admission, she died due to respiratory failure, without starting the treatment for advanced gastric cancer (*figure 1H*).

Although we knew there were anti-MDA5 autoantibodies present, the clinical course of the interstitial lung disease progression was too rapid to rescue. Anti-MDA5 antibody has been described as specific in patients with DM [6], and patients with this autoantibody have no or only mild muscular symptoms compared to patients with typical DM. The specific phenotype of palmar papules and cutaneous ulcerations is associated with this autoantibody in adult DM patients [7]. Our case had moderate muscular symptoms and palmar papules and it is noteworthy that the patient's respiratory status declined, while her muscular symptoms actually improved. Thus, we should pay close attention to respiratory status in DM patients who are anti-MDA5 autoantibody-positive.

Another feature in this case was that the serum ferritin level was elevated in parallel with exacerbation of the respiratory status. Ferritin, an iron-binding protein, regulates iron storage and homeostasis, as well as proinflammatory cytokine signaling [8]. Recently, high levels of ferritin have been associated with the development and prognosis of RP-ILD in patients with DM [9].

We report a rare case of RP-ILD and advanced gastric cancer in a patient with anti-MDA5 antibody-positive DM. Scrupulous attention to lethal RP-ILD must be given to patients with typical DM, even when complicating muscular disease has shown improvement. The DM patient described here, whose respiratory status was exacerbated in parallel with gradual rise of serum ferritin levels under combined modality therapy, is a dramatic clinical example of this need. ■

doi:10.1684/ejd.2014.2381

To cite this article: Yamaoka T, Doi C, Yokomi A, Tanemura A, Murota H, Tani M, Saruban H, Hamaguchi Y, Fujimoto M, Katayama I. Anti-MDA5 antibody-positive dermatomyositis with lethal progressive interstitial lung disease and advanced gastric cancer. *Eur J Dermatol* 2014 (epub ahead of print) doi:10.1684/ejd.2014.2381

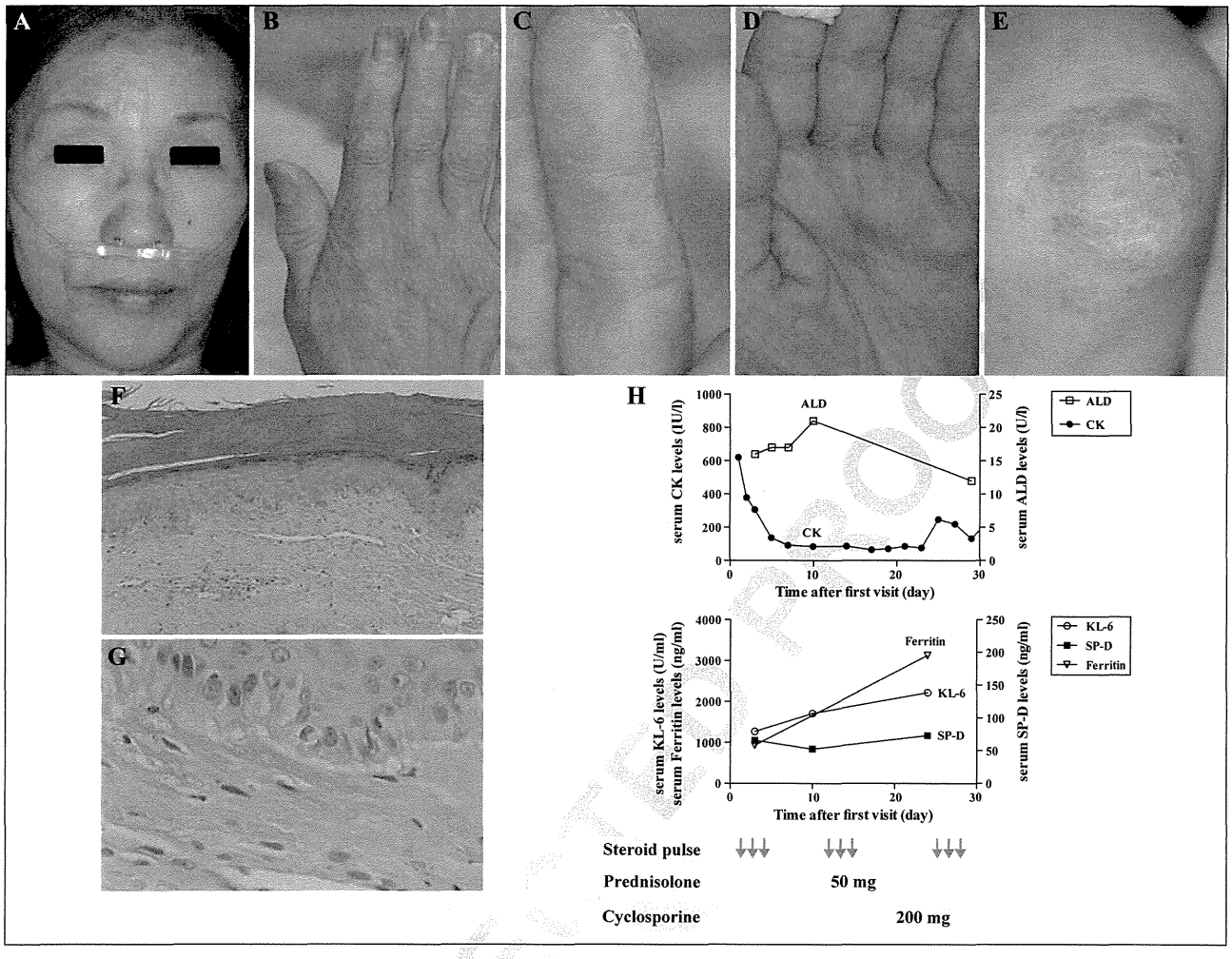

Figure 1. Clinical and histopathological findings, time course of medical treatments, and changes in laboratory data, before and after treatment. **A)** Skin lesions of the face, showing facial erythema with heliotrope rash. **B-E)** Discrete red-purple papules and/or erythematous macules appearing over the dorsal aspect of fingers, palms, and elbows. **F, G)** An atrophic epidermis with hyperkeratosis shows marked vacuolar alteration of basilar keratinocytes, associated with a sparse lymphocytic infiltration around superficial dermal vessels. **H)** Correlation between levels of serum markers and treatment with high-dose methylprednisolone (1 g/day intravenously for 3 days) and cyclosporine (5 mg/kg/day). It is important to note that levels of the muscle marker creatine kinase (CK) showed a gradual reduction, while those of the marker of interstitial lung disease, KL-6, increased. Hematoxylin and eosin staining; magnification in (F) ×40, and in (g) ×400.

Disclosure. *Financial support: none. Conflict of interest: none.*

[1] Department of Dermatology, Osaka University Graduate School of Medicine, 2-2 Yamadaoka, Suita, Osaka 565-0871, Japan
[2] Department of Dermatology, Higashiosaka City General Hospital, Osaka, Japan
[3] Department of Dermatology, Kanazawa University Graduate School of Medical Science, Kanazawa, Japan
<yamaoka@derma.med.osaka-u.ac.jp>

Toshifumi YAMAOKA[1]
Chie DOI[1]
Akinori YOKOMI[1]
Atsushi TANEMURA[1]
Hiroyuki MUROTA[1]
Mamori TANI[1]
Hiroko SARUBAN[2]
Yasuhito HAMAGUCHI[3]
Manabu FUJIMOTO[3]
Ichiro KATAYAMA[1]

1. Marie I, Hachulla E, Cherin P, *et al.* Interstitial lung disease in polymyositis and dermatomyositis. *Arthritis rheum* 2002; 47: 614-22.
2. Tsuchiya H, Tsuno H, Inoue M, *et al.* Mycophenolate mofetil therapy for rapidly progressive interstitial lung disease in a patient with clinically amyopathic dermatomyositis. *Mod Rheumatol* 2014; EarlyOnline: 1-3.
3. Sato S, Hoshino K, Satoh T, *et al.* RNA helicase encoded by melanoma differentiation-associated gene 5 is a major autoantigen in patients with clinically amyopathic dermatomyositis: Association with rapidly progressive interstitial lung disease. *Arthritis Rheum* 2009; 60: 2193-200.
4. Fujimoto M, Hamaguchi Y, Kaji K, *et al.* Myositis-specific anti-155/140 autoantibodies target transcription intermediary factor 1 family proteins. *Arthritis Rheum* 2012; 64: 513-22.
5. Kaji K, Fujimoto M, Hasegawa M, *et al.* Identification of a novel autoantibody reactive with 155 and 140 kDa nuclear proteins in patients with dermatomyositis: an association with malignancy. *Rheumatology* 2007; 46: 25-8.

6. Sato S, Hirakata M, Kuwana M, *et al.* Autoantibodies to a 140-kd polypeptide, CADM-140, in Japanese patients with clinically amyopathic dermatomyositis. *Arthritis Rheum* 2005; 52: 1571-6.
7. Fiorentino D, Chung L, Zwerner J, Rosen A, Casciola-Rosen L. The mucocutaneous and systemic phenotype of dermatomyositis patients with antibodies to MDA5 (CADM-140): a retrospective study. *J Am Acad Dermatol* 2011; 65: 25-34.
8. Kwak EL, Larochelle DA, Beaumont C, Torti SV, Torti FM. Role for NF-kappa B in the regulation of ferritin H by tumor necrosis factor-alpha. *J Biol Chem* 1995; 270: 15285-93.
9. Gono T, Sato S, Kawaguchi Y, *et al.* Anti-MDA5 antibody, ferritin and IL-18 are useful for the evaluation of response to treatment in interstitial lung disease with anti-MDA5 antibody-positive dermatomyositis. *Rheumatology* 2012; 51: 1563-70.
doi:10.1684/ejd.2014.2381

Journal of Medicinal Chemistry

Brief Article

pubs.acs.org/jmc

Identification of the Minimum Peptide from Mouse Myostatin Prodomain for Human Myostatin Inhibition

Kentaro Takayama,[†] Yuri Noguchi,[‡] Shin Aoki,[†] Shota Takayama,[†] Momoko Yoshida,[†] Tomo Asari,[†] Fumika Yakushiji,[†] Shin-ichiro Nishimatsu,[∥] Yutaka Ohsawa,[⊥] Fumiko Itoh,[‡] Yoichi Negishi,[§] Yoshihide Sunada,[⊥] and Yoshio Hayashi*[,†]

[†]Department of Medicinal Chemistry, [‡]Laboratory of Cardiovascular Medicine, and [§]Department of Drug Delivery and Molecular Biopharmaceutics, Tokyo University of Pharmacy and Life Sciences, Hachioji, Tokyo192-0392, Japan

[∥]Department of Molecular Biology and [⊥]Department of Neurology, Kawasaki Medical School, Kurashiki, Okayama 701-0192, Japan

Supporting Information

ABSTRACT: Myostatin, an endogenous negative regulator of skeletal muscle mass, is a therapeutic target for muscle atrophic disorders. Here, we identified minimum peptides **2** and **7** to effectively inhibit myostatin activity, which consist of 24 and 23 amino acids, respectively, derived from mouse myostatin prodomain. These peptides, which had the propensity to form α-helix structure, interacted to myostatin with K_D values of 30−36 nM. Moreover, peptide **2** significantly increased muscle mass in Duchenne muscular dystrophy model mice.

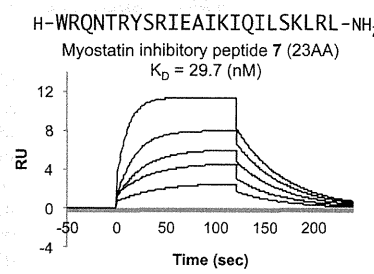

INTRODUCTION

Myostatin, also known as growth differentiation factor-8 (GDF-8), is a member of the transforming growth factor-β (TGF-β) superfamily proteins and contributes to adult muscle homeostasis as a negative regulatory factor of skeletal muscle growth.[1] The systemic overexpression of myostatin induces cachexia in mice,[2] but a loss of its function markedly increases muscle mass up to 2-fold in knockout mice.[1] These findings suggest that myostatin specific inhibitors enable the treatment of muscle atrophic disorders such as muscular dystrophy, cancer cachexia, sarcopenia, and disuse muscle atrophy. Therefore, several studies have attempted to develop myostatin inhibitors using antimyostatin antibodies or the soluble decoy receptors; for example, a neutralizing antibody of myostatin increased the muscle mass and strength in dystrophin-deficient Duchenne muscular dystrophy model (*mdx*) mice[3] and a soluble myostatin decoy receptor improved adverse effects such as loss of skeletal muscle and cardiac atrophy in tumor-bearing mice as well as cachexia.[4]

Similar to other TGF-β superfamily members, the myostatin precursor protein is cleaved in two during protein synthesis by a furin-like protease (i.e., the N-terminal prodomain and the C-terminal active domain).[5] Then mature myostatin, which is composed of the dimerized C-terminal domain by a disulfide bridge, can bind to activin type II receptors (ActRII). Binding results in the recruitment of type I receptors, ALK4 or ALK5 (ALK, activin receptor-like kinase), to stimulate the canonical Smad2 signaling pathway.[6−8]

Structural analysis has revealed that two separated N-terminal prodomains can assemble with the C-terminal homodimeric myostatin to form an inactive secreted complex, which is then stored in the extracellular matrix.[2,9] In circulation, the C-terminal dimeric myostatin is physiologically inactivated by some glycoproteins, such as follistatin and follistatin-like 3 (FSTL3).[10] Indeed, the externally administered FSTL3 as well as N-terminal prodomain inhibits myostatin.[5] Recently, Cash et al. demonstrated in 2012 that the N-terminal α-helical region of FSTL3 interacts with the type I receptor-binding site on myostatin.[11] Likewise, the N-terminal α-helical region of the prodomain in TGF-β1 binds to its own type I receptor-binding site, preventing receptor binding.[12] In this binding process, highly conserved Ile and Leu residues in the α-helical region contribute significantly to form an inactive complex between mature TGF-β1 and the prodomain (Figure 1A, underlined amino acid residues).[13]

On the basis of the findings of TGF-β1, myostatin inhibitors have been investigated with an emphasis on the myostatin prodomain sequence. For example, Jiang et al. reported that the glutathione S transferase-fusion protein bearing a 74 amino acid residue peptide derived from the N-terminal part of the human myostatin prodomain (position: 19−92 in the prodomain) significantly inhibits the myostatin activity.[14] In our investigations on the key peptide sequence responsible for selective myostatin inhibition from the same prodomain using a series of fusion proteins with the antibody Fc fragment, we found a short fragment sequence consisting of 29 amino acid residues located at positions 19−47 in the prodomain.[15] Intramuscular injection of this fragment peptide ameliorated not only muscle atrophy but also reduced muscle absolute force in the caveolin 3-

Received: July 31, 2014
Published: January 8, 2015

DOI: 10.1021/jm501170d
J. Med. Chem. 2015, 58, 1544−1549

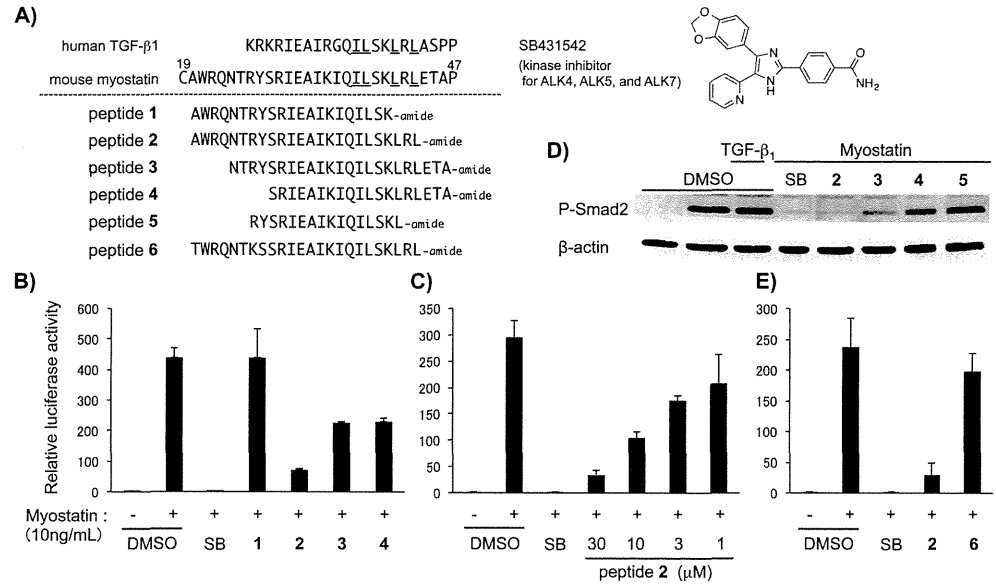

Figure 1. (A) Structures of peptides **1**–**6** and SB431542. Prodomain sequences of human TGF-β1 and mouse myostatin are shown at the top. Underline denotes highly conserved amino acids in the prodomain sequence of several TGF-β superfamily members. Numbers added to the top of an amino acid indicate the position of the prodomain sequence in mouse myostatin except for peptide **6** (human myostatin). (B) In vitro luciferase reporter assay to evaluate the human myostatin inhibitory activities of peptides **1**–**4**. (C) In vitro luciferase reporter assay to evaluate the dose-dependent inhibitory activity of peptides **2** on human myostatin. (D) Western blotting for phosphorylated Smad2 (P-Smad2) to evaluate the inhibitory activities of peptides **2**–**5** on myostatin signaling. (E) Human myostatin prodomain-derived peptide **6** corresponding to mouse-derived peptide **2** does not show a significant inhibitory activity to human myostatin in the luciferase reporter assay. Cell line, HepG2; peptide concentration, 30 μM (B,D,E); positive control (SB, SB431542) concentration, 5 μM; myostatin concentration, 10 ng/mL (0.4 nM); incubation, 8 h (B,C,E) or 1 h (D). Data (n = 3) are shown as means ± SD.

deficient limb-girdle muscular dystrophy 1C model mice. This sequence contains the sequence corresponding to the α-helical region of the aforementioned TGF-β1 prodomain, which is necessary to recognize mature TGF-β1 (Figure 1A).

In the present study to discover the minimum peptide sequence required to exhibit human myostatin inhibitory activity, a series of peptides based on 29 amino acid sequence derived from the mouse myostatin prodomain were synthesized using a 9-fluorenylmethoxycarbonyl (Fmoc)-based solid-phase peptide synthesis method and their antimyostatin activities were examined.

RESULTS AND DISCUSSION

First, we synthesized six peptides: mouse-derived peptides **1** (position: 20–40), **2** (position: 20–43), **3** (position: 24–46), **4** (position: 28–46), **5** (position: 26–41), and human-derived peptide **6** (position: 20–43). To evaluate whether these peptides affect the human myostatin-mediated downstream transcriptional response, we conducted transient transfection assays using a myostatin-responsive $(CAGA)_{12}$-luc reporter in HepG2 cells.[18] After preincubation of recombinant human myostatin with or without these peptides for 1 h in the culture medium, the mixture was added to HepG2 cells. Myostatin (10 ng/mL, 0.4 nM) induced strong reporter activities in this cellular assay (Figure 1B), but SB431542 (5 μM, Figure 1A), which is a potent kinase inhibitor for ALK4, ALK5, and ALK7,[19] completely blocked this myostatin-induced transcriptional activity. Among the synthesized peptides, peptide **2** (30 μM) showed a significant inhibitory activity (Figure 1B), which was dose dependent with an IC_{50} value of 4.1 μM (Figure 1C). Peptides **3** and **4**, in which several N-terminal amino acid residues from peptide **2** were truncated, exhibited weak inhibitory activities (Figure 1B). Peptide **1**, in which three C-terminal amino acid residues from peptide **2** were truncated, failed to show a significant inhibitory activity (Figure 1B). These results suggest that peptide **2** is one of the minimum effective sequences to elicit an inhibitory activity.

Next, the inhibitory effects of these peptides on Smad2 phosphorylation, which is induced by myostatin binding onto the activin type II receptor in HepG2 cells, were examined. The phosphorylation of Smad2 after 1 h of stimulation with myostatin was notably suppressed in the presence of not only SB431542 but also peptide **2** (Figure 1D). Peptides **3** and **4** showed weak and only a slight inhibition, respectively, which is consistent with the above-mentioned reporter assay (Figure 1B). In addition, shorter peptide **5**, which consisted entirely of a sequence corresponding to the critical α-helical region of the TGF-β1 prodomain for TGF-β1 binding proposed by Walton et al.,[13] did not affect the phosphorylation induced by myostatin (Figure 1D). These results indicated that the additional N- and C-terminal parts existing in peptide **2** compared to peptide **5** were important to induce the myostatin inhibitory activity. Intriguingly, it was noteworthy that peptide **6**, a human myostatin prodomain sequence corresponding to peptide **2** derived from a mouse sequence, did not show a significant inhibitory effect on human myostatin signaling (Figure 1E). This difference of inhibition between two species suggests that RY (positions 26 and 27 in the mouse prodomain) versus KS (positions 26 and 27 in the human prodomain) sequence is crucial for inhibiting the myostatin activity and human-derived prodomain might suppress the myostatin function with broader propeptide region because full-length or 74 amino acid residues prodomain peptides are known to inhibit myostatin activity.[14] This is probably the

DOI: 10.1021/jm501170d
J. Med. Chem. 2015, 58, 1544–1549

reason why any human-derived small peptide inhibitor (20–25 amino acid residues) has not been discovered to date. In this reporter assay, peptide **2** did not display any reporter activity in the absence of myostatin (Supporting Information (SI), Figure S1).

To more exactly determine the minimum peptide sequence that exerts an effective myostatin inhibitory activity, we synthesized a series of additional peptides **7**–**13** (Figure 2A)

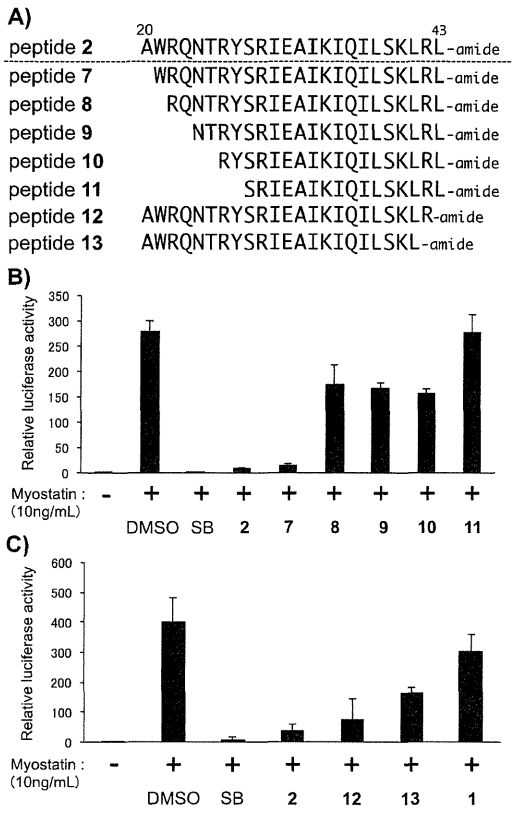

Figure 2. (A) Structures of shorter peptides **7**–**13**. Numbers added to the top of the amino acid indicate the position in the prodomain sequence of mouse myostatin. (B) In vitro luciferase reporter assay to evaluate the myostatin inhibitory activities of peptides **7**–**11** compared to that of peptide **2**. (C) In vitro luciferase reporter assay to evaluate the myostatin inhibitory activities of peptides **12** and **13** compared to those of peptides **1** and **2**. Cell line, HepG2; peptide concentration, 30 μM; positive control (SB, SB431542) concentration, 5 μM; myostatin concentration, 10 ng/mL (0.4 nM); incubation, 8 h. Data (n = 3) are shown as means ± SD.

and evaluated their inhibitory activities using the same reporter assay with HepG2 cells (Figure 2B). Peptide **7**, which lacks the N-terminal Ala residue (position 20 in the prodomain) from peptide **2**, showed a similar inhibitory activity as peptide **2**, indicating that the N-terminal Ala residue is not important for the myostatin inhibition. However, all other N-terminal truncated peptides **8**–**11** without the Trp residue at the 2-position (position 21 in the prodomain) in peptide **2** showed prominently weaker activities than peptides **2** and **7**, and no activity in the case of peptide **11** without RY sequence (positions 26 and 27). Additionally, N-terminal acetylated and C-terminal free peptides **7** (Ac-**7** and **7**-OH, respectively) exhibited the same inhibitory activities as peptide **7** (SI, Figure S2). These results suggest that the Trp residue at position 21 of the prodomain sequence, in addition to mouse-derived RY sequence at positions 26 and 27, plays an important role in the myostatin inhibitory activity.

On the other hand, the significance of the C-terminal amino acid residues on the inhibitory activity in peptide **2** was a little ambiguous. The inhibitory activity showed a gradual decrease according to the level of truncation from the C-terminus (Figure 2C). Namely compared to peptide **2**, peptides **12** or **13** (30 μM each) with a truncation of one (Leu) or two (Arg-Leu) amino acid residues showed 81 or 59% inhibition of the myostatin activity, respectively. As mentioned above, peptide **1** with a truncation of three amino acid residues lost its significant inhibitory activity. Although the observed weaker activity in these peptides might be attributed to not conserving the Leu residue (position 43 in case of myostatin prodomain), which is responsible for the TGF-β1 inactivation,[13] peptides **12** or **13** still have a significant inhibitory activity. Therefore, the minimum sequence required for myostatin recognition exists in position 21–42 or 21–43 of the prodomain sequence, and these sequences are not consistent with that necessary for TGF-β1 inactivation.[13] From these experiments, peptide **2** (position 20–43), which is consists of 24 amino acid residues, is the most potent small inhibitor among all the myostatin prodomain fragment peptides synthesized in the present study.

To understand the effect of the peptide secondary structure on the myostatin inhibitory activity, the circular dichroic (CD) spectra of peptides **2**–**5**, **7**, and **8** were measured in the absence or presence of 2,2,2-trifluoroethanol (TFE) because it is known that TFE generally promotes a helical structure formation of peptides.[20] Peptide **2** showed characteristic absorptions at 208 and 222 nm with increasing concentrations of TFE in 20 mM sodium phosphate buffer (pH 7.4), indicating that these peptides have the propensity to form an α-helix structure under at least 10% TFE-containing condition (Figure 3A). Peptide **3** did not display a typical α-helical nature, while less active peptides **4** or **5** in Figure 1 showed similar α-helicity compared with peptide **2**, respectively (SI, Figure S3A). In addition, N-terminal unprotected peptides **7** and **8** also exhibited the similar spectrum to peptide **2**, and N-terminal acetylation of these peptides (Ac-**7** and Ac-**8**) did not affect their secondary structures (SI, Figure S3B). Moreover, we synthesized peptide **2**-derived fragment peptides **2N** (AWRQNTRYSRIE-amide) and **2C** (AIKIQILSKLRL-amide) and their N-terminal acetylated peptides (Ac-**2N** and Ac-**2C**) to more precisely determine the structural property of peptide **2** and measured their CD spectra (SI, Figures S3C). The results indicate that the N-terminal part of peptide **2** (**2N**) has a random coiled structure, whereas the C-terminal part (**2C**) has the slight α-helical structure although peptide **2C** did not show any inhibitory activity (data not shown). Moreover, there was no influence of N-terminal acetylation to the peptide secondary structure (SI, Figure S3D).

Next, we performed surface plasmon resonance (SPR) assay to investigate the affinity of peptides **2**, **7**, and **8** to myostatin. Sensorgrams and their fitting curves of peptides were depicted in Figures 3B (peptide **2**) and SI, Figure S4 (peptides **7** and **8**), and the kinetic parameters [the binding dissociation constant (K_D) and the rate constants of association (k_{on}) and dissociation (k_{off})] of interaction with myostatin in respective peptides are described in Figure 3C. Myostatin inhibitory peptides **2** and **7** showed potent affinities to myostatin with K_D values of 35.9 and 29.7 nM, respectively (Figure 3C). These values were at least 3-fold higher affinity than less effective

DOI: 10.1021/jm501170d
J. Med. Chem. 2015, 58, 1544–1549

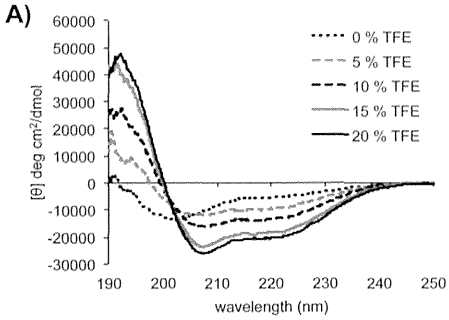

C)

	K_D (nM)	k_{on} ($M^{-1}s^{-1}$)	k_{off} (s^{-1})
peptide **2**	35.9	8.06×10^5	2.89×10^{-2}
peptide **7**	29.7	6.83×10^5	2.03×10^{-2}
peptide **8**	117	1.63×10^5	1.91×10^{-2}

Figure 3. (A) CD spectra of peptide **2** in the presence of 0–20% TFE solution prepared in 20 mM sodium phosphate buffer (pH 7.4); peptide concentration, 5 μM. (B) Sensorgrams and their fitting curves of peptide **2** to surface plasmon resonance (SPR) assay to analyze the affinity with myostatin; peptide concentrations, 6.25, 12.5, 25, 50, and 100 nM from the bottom sensorgram. Serial concentrations of peptides in HBS-P buffer (10 mM HEPES, pH 7.4, 300 mM NaCl, 0.005% (v/v) surfactant P20) were injected over myostatin-immobilized CM5 sensor chip. (C) Kinetic parameters of interaction with myostatin in peptides **2**, **7**, and **8**. The binding dissociation constant (K_D) and the rate constants of association (k_{on}) and dissociation (k_{off}) were determined with BIAevaluation software 3.0 from respective fitting curves based on sensorgrams.

peptide **8** lacking Trp residue at position 21 of the prodomain. These results correlate with the result of luciferase reporter assay shown in Figure 2, repeatedly suggesting that the Trp residue at position 21 plays an effective role in the direct binding of peptides **2** and **7** to myostatin for the significant inhibitory activity.

To further examine whether peptide **2** affects the weight of skeletal muscles in *mdx* mice (five week old males), we administrated 40 μL of the peptide solution (0.75 mM peptide **2** in saline) into the tibialis anterior (TA) muscle of the mice via an intramuscular injection. The treatments were repeated 2 weeks later in the same muscle. Then 4 weeks after the last treatment, the muscles were collected and weighed. Compared to muscles treated with saline, the weight of the treated muscles with the peptide showed 1.20 ± 0.03-fold increase (mean ± SD) (Figure 4), suggesting that inhibition of the myostatin function by peptide **2** can increase the weight of skeletal muscles in *mdx* mice as shown in previous reports.[21]

CONCLUSION

We synthesized a series of peptides derived from mouse myostatin prodomain. Peptides **2** and **7**, which consist of 24 and 23 amino acid residues, respectively, exhibited a potent myostatin inhibitory activity. Structure analysis revealed that

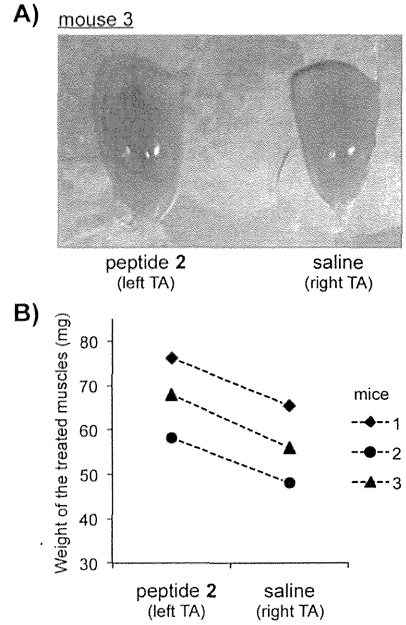

Figure 4. (A) Appearance of tibialis anterior (TA) muscles of *mdx* mice 3 after treatment with peptide **2** (left TA) or the vehicle (saline, right TA). Peptide solution (40 μL, 0.75 mM peptide **2** in saline) was intramuscularly injected into the tibialis anterior muscle of respective mice 1–3. Treatment was repeated 2 weeks later in the same muscle. Their muscles were collected and weighed 4 weeks after the last treatment. (B) Weight of the treated muscles in respective mice 1–3 (n = 3).

these peptides have the propensity to form α-helical structures in the presence of at least 10% TFE. Moreover, Trp residue (position 21) and mouse-derived RY sequence (positions 26 and 27) in the N-terminal random coiled parts in these peptides played an important role in the effective myostatin inhibition as well as their C-terminal α-helical region that was identical between mouse and human sequences. Further biological evaluations revealed that peptide **2** significantly increased muscle mass (about 20%) in Duchenne muscular dystrophy model mice. In the future, we plan to conduct a detailed structure–activity relationship study based on peptide **7** to obtain a more potent inhibitor and a long-lasting activity in vivo.

EXPERIMENTAL SECTION

Reagents and solvents were purchased from Wako Pure Chemical Industries (Osaka, Japan), Sigma-Aldrich (St. Louis, MO), Watanabe Chemical Industries (Hiroshima, Japan), and Tokyo Chemical Industries (Tokyo, Japan). All were used as received. Sterile Dulbecco's Modified Eagle's Medium (DMEM) and fetal bovine serum (FBS) were purchased from Nacalai Tesque (Kyoto, Japan) and Life Technologies (Carlsbad, CA), respectively. Sterile 100 mm dishes and 24/96-well clear/white-wall plates were purchased from Iwaki (Tokyo, Japan) and Corning (Cambridge, MA), respectively. Polyethylenimine (PEI) transfection reagents were purchased from Polysciences (Warrington, PA).

1. Synthesis of Peptide Derivatives. As previously reported,[16,17] the Fmoc-NH-SAL resin (50–100 mg, 0.028–0.047 mmol) and Fmoc-amino acids (0.084–0.141 mmol) were sequentially coupled using the *N,N'*-diisopropylcarbodiimide (DIPCI, 0.084–0.141 mmol)-1-hydroxybenzotriazole (HOBt, 0.084–0.141 mmol) method for 2–3 h in DMF (1.0 mL) after removing each Fmoc group with 20% piperidine-*N,N'*-dimethylformamide (DMF) (1.5 mL, 20 min) to

DOI: 10.1021/jm501170d
J. Med. Chem. 2015, 58, 1544–1549

obtain protected peptide- resins. The resins were treated with TFA–*m*-cresol–thioanisole–EDT (4.0 mL, 40:1:1:1) for 150 min at rt. The TFA salts of peptides **1**–**13** were obtained by preparative RP-HPLC purification in a 0.1% aqueous TFA–CH_3CN system and solubilized in dimethyl sulfoxide (DMSO) as 3 mM stock solutions for biological evaluation. High-resolution mass spectra (TOF MS ES+) were recorded on a micromass LCT (see SI). The synthesized peptides were >95% pure (RP-HPLC analysis at 230 nm, see SI).

2. Luciferase Reporter Assay. HepG2 cells were cultured in DMEM (Nacalai Tesque) containing 10% FBS (Life Technologies) and nonessential amino acids (Sigma). The cells were seeded at 7.5×10^4 cells per well in the 24-well plates the day before transfection. The cells were transfected using polyethylenimine (Polysciences). After 28 h of transfection, the medium was exchanged to DMEM containing 0.3% FBS, and the cells were incubated for 18 h at 37 °C under 5% CO_2. Each synthesized peptide was dissolved with DMSO, diluted by adding DMEM containing recombinant myostatin (Wako) and 0.3% FBS (final concentration: 30 μM peptide, 10 ng/mL (0.4 nM) myostatin, and 1% DMSO), and incubated for 1 h. Cells were treated with a peptide solution and incubated at 37 °C under 5% CO_2. After 8 h, cells were washed with PBS. The lysates were prepared, and the luciferase activity was measured using a luciferase assay system (Promega, Madison, WI, USA) according to the standard protocol. SB431542 (Wako) was used as a positive control and underwent the same manipulation (final concentration, 5 μM). The results were corrected for the β-galactosidase activity (pCH110; GE Healthcare). Each experiment was carried out in triplicate. Values are presented as the mean ± SD (n = 3).

3. Western Blotting. HepG2 cells were seeded at 1.5×10^5 cells per well in 12-well plates and incubated for 24 h. The medium was exchanged to DMEM containing 0.3% FBS, and cells were incubated for 18 h at 37 °C under 5% CO_2. Each synthesized peptide was dissolved with DMSO, diluted by adding DMEM containing myostatin (Wako) and 0.3% FBS (final concentration; 30 μM peptide, 10 ng/mL (0.4 nM) myostatin and 1% DMSO), and incubated for 1 h. Cells were treated with the peptide solution and incubated at 37 °C under 5% CO_2. After 1 h, cells were washed with PBS and lysed in 200 μL of TNE buffer [10 mM Tris (pH 7.4), 150 mM NaCl, 1 mM EDTA, 1% Nonidet P-40, 1 mM PMSF, 5 μg/mL leupeptin, 30 unit/mL aprotinin, 2 mM sodium vanadate, 40 mM NaF, and 20 mM β-glycerophosphate]. The lysates were boiled for 5 min in sample buffer, separated by sodium dodecyl sulfate–polyaclylamide electrophoresis (SDS-PAGE) in 8% polyacrylamide gels, and transferred to Hybond-C extra membranes (GE healthcare). The membrane was probed with primary antibodies; antiphosphorylated Smad2 (×2000, our own make) or antiβ-actin (×4000, Sigma). The primary antibodies were detected with horseradish peroxidase conjugated secondary antibodies and chemiluminescent substrate (Pierce) and visualized with imaging system (Image Quant LAS-4000, GE-healthcare).

4. Measurement of the Circular Dichroic Spectra. CD spectra of the synthetic peptides were obtained at 25 °C using a Jasco J-1500 CD spectrometer (JASCO, Japan) in a quartz cell with a 0.5 cm path length. Spectra were collected between 190–250 nm with a scan speed of 100 nm/min, a response time of 1 s, and a bandwidth of 1 nm. Peptide samples with a final concentration of 5 μM were prepared in 20 mM sodium phosphate buffer (pH 7.4) containing 0–20% 2,2,2-trifluoroethanol (TFE). The baseline scan, which was acquired by measuring the buffer alone, was subtracted from the experimental readings. CD data, which were collected every 0.1 nm, were the average of nine scans. The normalized CD data was expressed in the mean residue ellipticity (deg cm^2 $dmol^{-1}$) and plotted as functions of wavelength.

5. Surface Plasmon Resonance (SPR) Assay. The binding dissociation constant K_D, the association rate constant k_{on}, and the dissociation rate constant k_{off} of peptides were determined by SPR using Biacore X (GE Healthcare). Recombinant myostatin, (carrier-free, R&D Systems) was dissolved in 10 mM sodium acetate (pH 5.5) at a final concentration of 1 μg/mL and immobilized onto CM5 sensor chip activated by the amine coupling kit (GE Healthcare) according to the instruction. About 650 response units (RU) of myostatin were coupled to flow cell 2. Flow cell 1 was not treated at all and was served as a reference. Each peptide was diluted in HBS-P buffer (10 mM HEPES, pH 7.4, 300 mM NaCl, 0.005% (v/v) surfactant P20), which was also used as running buffer. A serial concentrations of peptides were injected at 25 °C and a flow rate of 20 μL/min. Association and dissociation were measured over 120 s; 1 M NaCl was used for regeneration. To determine each parameter, BIAevaluation software 4.1 was used. All sensorgrams were fitted to a 1:1 (Langmuir) binding model.

6. Intramuscular Administration of Peptide 2 into Anterior Tibialis of *mdx* Mice. Animal studies were approved by the Animal Research Committee of Tokyo University of Pharmacy and Life Sciences. Peptide solution (40 μL of the 0.75 mM peptide **2** in saline) and saline (control) were intramuscularly injected into left and right tibialis anterior muscle of 5-week-old *mdx* mice, respectively. After 2 weeks, the treatment was repeated for the same muscle. Then 4 weeks after the last treatment, the muscles were collected and weighed.

■ ASSOCIATED CONTENT

Ⓢ Supporting Information

Analytical data for all peptide derivatives, analytical HPLC chromatograms, and Figures S1–S4. This material is available free of charge via the Internet at http://pubs.acs.org.

■ AUTHOR INFORMATION

Corresponding Author

*Phone: +81 42 676 3275. Fax: +81 42 676 3279. E-mail: yhayashi@toyaku.ac.jp. Address: Department of Medicinal Chemistry, Tokyo University of Pharmacy and Life Sciences, Tokyo 192-0392, Japan.

Notes

The authors declare no competing financial interest.

■ ACKNOWLEDGMENTS

This research was supported by Grants from the Ministry of Education, Culture, Sports, Science and Technology (MEXT) of Japan, including a Grant-in-Aid for Scientific Research (B) 23390029 (Y.H.), Platform for Drug Discovery, Informatics and Structural Life Science (Y.H.), an Intramural Research Grant (26-8) for Neurological and Psychiatric Disorders on NCNP (Y.H. and Y.S.), and a Grant-in-Aid for Creative Research for Intellectual Property from Tokyo University of Pharmacy and Life Sciences (K.T.). We thank Akari Nakamura, Yusuke Saga, and Yuko Sohma for peptide synthesis.

■ ABBREVIATIONS USED

ActRII, activin type II receptor; CD, circular dichroic; DIPCI, *N*,*N*′-diisopropylcarbodiimide; DMEM, Dulbecco's Modified Eagle's Medium; DMF, *N*,*N*′-dimethylformamide; DMSO, dimethyl sulfoxide; EDT, 1,2-ethanedithiol; ES, electrospray; FBS, fetal bovine serum; Fmoc, 9-fluorenylmethoxycarbonyl; FSTL3, follistatin-like 3; GDF-8, growth differentiation factor-8; HEPES, 4-(2-hydroxyethyl)-1-piperazineethanesulfonic acid; HOBt, 1-hydroxybenzotriazole; K_D, binding dissociation constant; k_{on}, association rate constant; k_{off}, dissociation rate constant; MS, mass spectrometry; RP-HPLC, reversed-phase high-performance liquid chromatography; PEI, polyethylenimine; P-Smad2, phosphorylated Smad2; SDS-PAGE, sodium dodecyl sulfate–polyacylamide electrophoresis; SPPS, solid-phase peptide synthesis; SPR, surface plasmon resonance; TA, tibialis anterior; TFA, trifluoroacetic acid; TFE, 2,2,2-trifluoroethanol; TGF-β, transforming growth factor-β; TOF, time-of-flight

DOI: 10.1021/jm501170d
J. Med. Chem. 2015, 58, 1544–1549

REFERENCES

(1) McPherron, A. C.; Lawler, A. M.; Lee, S.-J. Regulation of skeletal muscle in mice by a new TGF-β superfamily member. *Nature* **1997**, *387*, 83−90.

(2) Zimmers, T. A.; Davies, M. V.; Koniaris, L. G.; Haynes, P.; Esquela, A. F.; Tomkinson, K. N.; McPherron, A. C.; Wolfman, N. M.; Lee, S.-J. Induction of cachexia in mice by systemically administrated myostatin. *Science* **2002**, *296*, 1486−1488.

(3) Bogdanovich, S.; Krag, T. O.; Barton, E. R.; Morris, L. D.; Whittemore, L. A.; Ahima, R. S.; Khurans, T. S. Functional improvement of dystrophic muscle by myostatin blockade. *Nature* **2002**, *420*, 418−421.

(4) Zhou, X.; Wang, J. L.; Lu, J.; Song, Y.; Kwak, K. S.; Jiao, Q.; Rosenfeld, R.; Chen, Q.; Boone, T.; Scott Simonet, W.; Lacey, D. L.; Goldberg, A. L.; Han, H. Q. Reversal of cancer cachexia and muscle wasting by ActRIIB antagonism leads to prolonged survival. *Cell* **2010**, *142*, 531−543.

(5) Lee, S.-J.; McPherron, A. C. Regulation of myostatin activity and muscle growth. *Proc. Natl. Acad. Sci. U. S. A.* **2001**, *98*, 9306−9311.

(6) Wrana, J. L.; Attisano, L.; Wieser, R.; Ventura, F.; Massagué, J. Mechanism of activation of the TGF-β receptor. *Nature* **1994**, *370*, 341−347.

(7) Wolfman, N. M.; McPherron, A. C.; Pappano, W. M.; Davies, M. V.; Song, K.; Tomkinson, K. N.; Wright, J. F.; Zhao, L.; Sebald, S. M.; Greenspan, D. S.; Lee, S.-J. Activation of latent myostatin by the BMP-1/tolloid family of metalloproteinases. *Proc. Natl. Acad. Sci. U. S. A.* **2003**, *100*, 15842−15846.

(8) Hinck, A. P. Structural studies of the TGF-βs and their receptors—insights into evolution of the TGF-β superfamily. *FEBS Lett.* **2012**, *586*, 1860−1870.

(9) Anderson, S. B.; Goldberg, A. L.; Whitman, M. Identification of a novel pool of extracellular pro-myostatin in skeletal muscle. *J. Biol. Chem.* **2008**, *283*, 7027−7035.

(10) Hill, J. J.; Davies, M. V.; Pearson, A. A.; Wang, J. W.; Hewick, R. M.; Wolfman, N. M.; Qiu, Y. The myostatin propeptide and the follistatin-related gene are inhibitory binding proteins of myostatin in normal serum. *J. Biol. Chem.* **2002**, *277*, 40735−40741.

(11) Cash, J. N.; Angerman, E. B.; Kattamuri, C.; Nolan, K.; Zhao, H.; Sidis, Y.; Keutmann, H. T.; Thompson, T. B. Structure of myostatin·follistatin-like 3: N-terminal domains of follistatin-type molecules exhibit alternate mode of binding. *J. Biol. Chem.* **2012**, *287*, 1043−1053.

(12) Shi, M.; Zhu, J.; Wang, R.; Chen, X.; Mi, L.; Walz, T.; Springer, T. A. Latent TGF-β structure and activation. *Nature* **2011**, *474*, 343−349.

(13) Walton, K. L.; Makanji, Y.; Chen, J.; Wilce, M. C.; Chan, K. L.; Robertson, D. M.; Harrison, C. A. Two distinct region of latency-associated peptide coordinate stability of the latent transforming growth factor-β1 complex. *J. Biol. Chem.* **2010**, *285*, 17029−17037.

(14) Jiang, M.-S.; Liang, L.; Wang, S.; Ratovitski, T.; Holmstrom, J.; Barker, C.; Stotish, R. Characterization and identification of the inhibitory domain of GDF-8 propeptide. *Biochem. Biophys. Res. Commun.* **2004**, *315*, 525−531.

(15) Ohsawa, Y.; Takayama, K.; Nishimatsu, S.; Okada, T.; Fujino, M.; Fukai, Y.; Murakami, T.; Hagiwara, H.; Itoh, F.; Tsuchida, K.; Hayashi, Y.; Sunada Y. *unpublished results.*

(16) Takayama, K.; Suehisa, Y.; Fujita, T.; Nguyen, J.-T.; Futaki, S.; Yamamoto, A.; Kiso, Y.; Hayashi, Y. Oligoarginine-based prodrugs with self-cleavable spacers for caco-2 cell permeation. *Chem. Pharm. Bull.* **2008**, *56*, 1515−1520.

(17) Sohma, Y.; Sasaki, M.; Hayashi, Y.; Kimura, T.; Kiso, Y. Novel and efficient synthesis of difficult sequence-containing peptides through O−N intramolecular acyl migration reaction of *O*-acyl isopeptides. *Chem. Commun.* **2004**, *1*, 124−125.

(18) Dennler, S.; Itoh, S.; Vivien, D.; Dijke, P.; Huet, S.; Gauthier, J.-M. Direct binding of Smad3 and Smad4 to critical TGF β-inducible elements in the promoter of human plasminogen activator inhibitor-type 1 gene. *EMBO J.* **1998**, *17*, 3091−3100.

(19) Callahan, J. F.; Burgess, J. L.; Fornwald, J. A.; Gaster, L. M.; Harling, J. D.; Harrington, F. P.; Heer, J.; Kwon, C.; Lehr, R.; Mathur, A.; Olson, B. A.; Weinstock, J.; Laping, N. J. Identification of novel inhibitors of the transforming growth factor β1 (TGF-β1) type 1 receptor (ALK5). *J. Med. Chem.* **2002**, *45*, 999−1001.

(20) Roccatano, D.; Colombo, G.; Fioroni, M.; Mark, A. E. Mechanism by which 2,2,2-trifluoroethanol/water mixtures stabilize secondary-structure formation in peptides: a molecular dynamics study. *Proc. Natl. Acad. Sci. U. S. A.* **2002**, *99*, 12179−12184.

(21) Nakatani, M.; Takehara, Y.; Sugino, H.; Matsumoto, M.; Hashimoto, O.; Hasegawa, Y.; Murakami, T.; Uezumi, A.; Takeda, S.; Noji, S.; Sunada, Y.; Tsuchida, K. Transgenic expression of a myostatin inhibitor derived from follistatin increases skeletal muscle mass and ameliorates dystrophic pathology in mdx mice. *FASEB J.* **2008**, *222*, 477−487.

DOI: 10.1021/jm501170d
J. Med. Chem. 2015, 58, 1544−1549

RHEUMATOLOGY

Rheumatology 2014;53:2196–2203
doi:10.1093/rheumatology/keu258
Advance Access publication 26 June 2014

Original article

Cytokine profiles in polymyositis and dermatomyositis complicated by rapidly progressive or chronic interstitial lung disease

Takahisa Gono[1], Hirotaka Kaneko[1], Yasushi Kawaguchi[1], Masanori Hanaoka[1], Sayuri Kataoka[1], Masataka Kuwana[2], Kae Takagi[1], Hisae Ichida[1], Yasuhiro Katsumata[1], Yuko Ota[1], Hidenaga Kawasumi[1] and Hisashi Yamanaka[1]

Abstract

Objective. PM and DM are often complicated by interstitial lung disease (ILD). In this study we aimed to evaluate various serum cytokines in patients with PM/DM with ILD so as to clarify the differences in pathophysiology between anti-melanoma differentiation-associated gene 5 antibody-associated ILD (anti-MDA5-ILD) and anti-aminoacyl tRNA synthetase antibody-associated ILD (anti-ARS-ILD).

Methods. We evaluated the serum cytokine profiles of 38 patients with PM/DM and compared the cytokine profiles of the non-ILD and ILD subsets as well as the anti-MDA5-ILD and anti-ARS-ILD subsets.

Results. The myositis intention-to-treat activity index score, which indicates whole disease activity, significantly correlated with serum IL-6, IL-8, TNF-α and IP-10. These cytokine levels were significantly higher in the ILD subset than the non-ILD subset and were lower in the ILD subset following treatment. By multivariate analysis, TNF-α was the most significant cytokine [$P = 0.0006$, odds ratio (OR) 1.4, CI 1.1, 2.2] associated with PM/DM with ILD. IL-8 levels were significantly higher in anti-MDA5-ILD than in anti-ARS-ILD, although IL-6, TNF-α and IP-10 levels were high in both subsets. IL-8 was the most significant cytokine ($P = 0.0006$, OR 1.5, CI 1.1, 3.0) associated with anti-MDA5-ILD by multivariate analysis. Moreover, the ratio of IL-4 to IFN-γ was lower in anti-MDA5-ILD than in anti-ARS-ILD.

Conclusion. IL-6, IL-8, TNF-α and IP-10 are associated with global disease activity in PM/DM. These cytokine levels were high, especially in the ILD subset. Serum IL-8 levels and the balance between IL-4 and IFN-γ may contribute to the differences in pathophysiology between anti-ARS-ILD and anti-MDA5-ILD.

Key words: polymyositis, dermatomyositis, interstitial lung disease, TNF-α, IL-6, IL-8.

Introduction

PM and DM are idiopathic inflammatory myopathies that are characterized by inflammation of the muscles, skin, lungs and heart [1, 2]. PM and DM are classified as autoimmune diseases because several types of myositis-specific autoantibody (MSA) are detected and immunosuppressive therapy such as corticosteroids is effective [3]. PM and DM are occasionally complicated by interstitial lung disease (ILD) [4]. ILD is one of the prognostic factors in PM/DM [5].

With regard to cytokines, IL-1α, IL-1β, IL-18, TNF-α, IFN-α and IFN-γ are highly expressed in the muscle tissues of PM/DM patients [6]. Dendritic cells, macrophages, lymphocytes, muscle fibres and endothelial cells of capillaries synthesize these cytokines in the muscle tissues of patients with PM/DM. In ILD with PM/DM, it has been reported that serum CRP and the IFN-γ-inducible chemokines C-X-C motif ligand 9 (CXCL9) and CXCL10 are associated with anti-Jo-1 antibody-associated ILD in which myositis is frequently

[1]Institute of Rheumatology, Tokyo Women's Medical University and [2]Division of Rheumatology, Department of Internal Medicine, Keio University School of Medicine, Tokyo, Japan.

Submitted 3 September 2013; revised version accepted 2 May 2014.

Correspondence to: Yasushi Kawaguchi, Institute of Rheumatology, Tokyo Women's Medical University, 10-22 Kawada-cho, Shinjuku-Ku, Tokyo 162-0054, Japan. E-mail: y-kawa@ior.twmu.ac.jp

complicated [7]. Serum biomarkers such as cytokines and chemokines could be affected by the whole disease status, including myositis, dermatitis and ILD, in PM/DM. However, the precise differences in the cytokine profiles between myositis and ILD in PM/DM remain unknown.

In PM/DM, complication with ILD is associated with anti-aminoacyl-tRNA synthetase (ARS), including Jo-1 antibody or anti-melanoma differentiation-associated gene 5 (MDA5) antibody [4, 8]. In particular, rapidly progressive ILD (RP-ILD) is an intractable and life-threatening complication. Clinically amyopathic DM (CADM) patients with anti-MDA5 antibodies have frequent complications with RP-ILD, especially in Japan [9–11], where it is classified as acute interstitial pneumonia and reflects diffuse alveolar damage upon pathological examination. In contrast, chronic ILD is frequently observed in anti-ARS antibody-associated PM/DM, which responds well to treatment with corticosteroids. The response to treatment and the mortality rate are different between anti-MDA5 antibody-associated ILD (anti-MDA5-ILD) and anti-ARS antibody-associated ILD (anti-ARS-ILD) [4]. Hyperferritinaemia is usually revealed in RP-ILD with anti-MDA5 antibodies but not in anti-ARS antibody ILD [10, 11]. Although the pathogenesis of RP-ILD with anti-MDA5 antibodies has been tentatively attributed to a cytokine storm triggered by a viral infection, especially in the skin and lungs, its exact mechanism is unknown [10, 12]. In addition, the differences in pathophysiology between these two antibody-associated ILD subsets remain unknown.

Therefore we investigated the characteristics of the cytokine profiles in PM/DM with and without ILD. In addition, we compared the cytokine profiles of anti-MDA5 antibody ILD and anti-ARS antibody ILD and clarified the differences in pathophysiology between these two subsets of patients.

Patients and methods

Patients

In this study, patients who were admitted to Tokyo Women's Medical University Aoyama Hospital from 1992 to 2010 were retrospectively examined. We found that 124 patients had been diagnosed with PM, DM or CADM. Of these 124 patients, 78 and 46, respectively, were complicated with and without ILD. Of the 78 patients with ILD, anti-ARS antibodies and anti-MDA5 antibodies were detected in 17 and 14, respectively. To clarify the differences in pathophysiology and cytokine profile between anti-MDA5 antibody ILD and anti-ARS antibody ILD, patients without either anti-MDA5 or anti-ARS were not enrolled in this study. Serum samples were obtained from 11 anti-ARS antibody-positive patients and 10 anti-MDA5 antibody-positive patients. Of 46 patients without ILD, sera were obtained from 17 patients. In 10 patients with anti-MDA5 antibody ILD or anti-ARS antibody ILD and 29 without ILD, the volume of the serum samples was too small to measure various cytokines. These 38 patients were enrolled in the present study. They were diagnosed as having PM/DM or CADM based on the criteria of Bohan and Peter [13] or Sontheimer [14], respectively. Specific rashes, including heliotrope rash, Gottron's sign or Gottron's papules, were used to define DM and CADM. In general, CADM patients present with typical skin lesions and amyopathy or hypomyopathy for >6 months. A subset of the CADM group in this study included patients who developed ILD within the first 6 months of the study. All of the 38 enrolled patients suffered from skin rashes, myopathy or respiratory symptoms (or a combination thereof).

In all of the enrolled patients, disease status was active upon admission, so the physicians decided to begin immunosuppressive therapy or to increase the intensity of therapy, such as treating with intermediate or high-dose prednisolone or adding additional immunosuppressive agents. Disease duration was defined as the time between the appearance of PM/DM-associated symptoms and admission. The clinical data were obtained from medical records at the time the serum samples were obtained. In addition, serum was obtained from 15 healthy controls (HCs). This study was approved by the ethical committee of Tokyo Women's Medical University. All patients and controls provided written informed consent according to the Declaration of Helsinki.

Evaluation of muscular and extra-muscular manifestations

Myositis was evaluated by manual muscle testing, creatine kinase (CK) and electromyography. MRI and muscle biopsy of the extremities was carried out if necessary. Dermatitis and arthritis were evaluated by physical examination. If necessary, dermatologists evaluated the skin eruptions and performed a skin biopsy. Pulmonary disease was assessed by chest radiography and high-resolution CT. Pulmonary function was also evaluated if findings were revealed in the lung. Cardiac function was evaluated by electrocardiography and echocardiography. Scintigram and myocardial biopsy were conducted if necessary. Enteropathy was assessed by gastrointestinal endoscopy and colonoscopy. A malignancy survey was performed for all of the patients.

Evaluation of pulmonary function and classification of ILD

Pulmonary function was evaluated from the arterial oxygen tension (PaO_2)/fractional inspired oxygen (F_iO_2) ratio (i.e. P/F ratio), alveolar–arterial oxygen difference ($A\text{-}aDO_2$) and vital capacity percentage (%VC). RP-ILD was defined as a progressive dyspnoea that developed rapidly, over days to weeks, after the onset of respiratory symptoms. Chronic ILD was defined as a progressive dyspnoea that developed slowly, over months [15, 16].

Evaluation of disease activity for PM/DM/CADM

Disease activity was evaluated using the myositis disease activity core set, which the International Myositis Assessment and Clinical Studies (IMACS) group has proposed and recommended [3, 17, 18]. Muscular symptoms

and extra-muscular complications were measured using the myositis activity assessment visual analogue scales (MYOACT) and the myositis intention-to-treat activity index (MITAX). Constitutional, cutaneous, skeletal, gastrointestinal, pulmonary, cardiac and muscular disease activity were included in both the MYOACT and MITAX. The MITAX score was the MITAX sum score divided by the total score of 63 points. The details of clinical information required for the estimation of MITAX and MYOACT were available in the medical records. The MITAX and MYOACT were estimated retrospectively by physicians in charge or evaluators who were blinded to the results of cytokine profiles in reference to the medical records information.

Evaluation of MSAs

Anti-MDA5 antibody was detected with the use of an ELISA using recombinant MDA5 as an antigen, as described previously [9]. Anti-ARS antibodies, including Jo-1, EJ, PL-7, PL-12 and OJ, were measured with RNA immunoprecipitation assays. The other MSAs were detected through immunoblots using the Myositis Profile Euroline antibody test system for the *in vitro* determination of antibodies against myositis-associated antigens in human serum (Euroimmun, Lübeck, Germany).

Measurement of cytokines

Serum samples were stored at −80°C. The levels of serum cytokines, including IL-1β, IL-2, IL-4, IL-6, IL-8, IL-10, IL-12, IL-13, IL-17, TNF-α, IFN-α, IFN-γ and IFN-γ-inducible 10-kDa (IP-10), were measured by multiplex assay using the Milliplex MAP Human Cytokine/Chemokine Panel (EMD Millipore, Waltham, MA, USA), Bio-Plex 200 System and Bio-Plex Manager software version 6.0 (Bio-Rad Laboratories, Hercules, CA, USA).

Statistical analysis

Statistical analyses were performed using the chi-square test for the comparison of frequencies, Fisher's exact test was used when appropriate and the Mann–Whitney *U* test was used for the comparison of median values. Correlation coefficients were established by employing Spearman's correlation coefficients. Multiple linear regression analysis was performed when appropriate. The Wilcoxon signed-rank test was performed when comparing the cytokine levels of patients with active ILD and the cytokine levels after improvement. The data were analysed using JMP software (SAS Institute, Cary, NC, USA). *P*-values <0.05 indicated statistical significance.

Results

Clinical characteristics of the enrolled patients

A total of 38 patients was enrolled in this study (Table 1). The median age was 52 years and 74% of the participants were female. The number of PM, DM and CADM cases was 12, 14 and 12, respectively. The median disease duration was 4 months. The frequency of ILD, cardiomyopathy and malignancy was 55%, 13% and 3%, respectively. The positivity rate of anti-ARS antibody, anti-Mi-2 antibody, anti-MDA5 antibody and anti-signal recognition particle (SRP) antibody was 32%, 3%, 26% and 5%, respectively. The median MITAX score was 0.19.

Comparison of cytokine levels in PM/DM/CADM and HCs

To investigate the characteristics of cytokine profiles in all of the PM/DM/CADM patients, the levels of each cytokine were compared in PM/DM/CADM patients and the HCs (Table 2). Serum IL-1β, IL-2, IL-4, IL-6, IL-8, IL-10, TNF-α, IFN-α, IFN-γ and IP-10 were significantly higher in PM/DM/CADM patients than HCs. IL-12, IL-13 and IL-17 levels did not differ between PM/DM/CADM patients and HCs.

Correlations between each cytokine level in PM/DM/CADM

We estimated the correlations between each cytokine level in PM/DM/CADM. As shown in Table 3, IL-1β levels were significantly ($P < 0.001$) correlated with the levels of IL-2, IL-6, IL-12 and IFN-γ. Moreover, the correlation between IL-2 and IL-12 and between IL-6 and TNF-α was significant ($P < 0.001$). IL-10 levels were significantly ($P < 0.001$) correlated with the levels of TNF-α, IFN-γ and IP-10.

Correlation between cytokine levels and whole disease activity

We evaluated the association between each cytokine level and the MITAX score, which is an indicator of both muscular and extra-muscular disease activity. The MITAX score was significantly correlated with the level of IL-6 ($r_s = 0.59$, $P < 0.0001$), IL-8 ($r_s = 0.34$, $P < 0.05$), IL-10 ($r_s = 0.36$, $P < 0.05$), TNF-α ($r_s = 0.53$, $P < 0.0001$) and IP-10 ($r_s = 0.35$, $P < 0.05$).

Table 1 Clinical characteristics of the enrolled patients

Age, median (IQR), years	52 (39–58)
Female, *n* (%)	28 (74)
PM, DM, CADM, *n*	12, 14, 12
Disease duration, median (IQR), months	4 (2–7)
ILD, *n* (%)	21 (55)
Cardiomyopathy, *n* (%)	5 (13)
Malignancy, *n* (%)	1 (3)
Myositis specific autoantibodies, *n* (%)	
Anti-ARS	12 (32)
Anti-Mi-2	1 (3)
Anti-MDA5	10 (26)
Anti-SRP	2 (5)
MITAX, median (IQR)	0.19 (0.11–0.30)

A total of 38 patients were enrolled in the present study. IQR: interquartile range; ILD: interstitial lung disease; CADM: clinically amyopathic DM; ARS: aminoacyl-tRNA synthetase; MDA5, melanoma differentiation-associated gene 5; SRP: signal recognition particle; MITAX: myositis intention-to-treat activity index.

Comparison of clinical characteristics of the non-ILD subset and the ILD subset

To investigate the cytokine profiles in PM/DM/CADM-associated ILD, clinical characteristics and cytokine levels were compared between the non-complicating ILD (non-ILD) subset and the ILD subset (Table 4). Regarding the differences between the two subsets, the constitutional visual analogue scale (VAS), cutaneous VAS and MITAX scores were higher in the ILD subset than in the non-ILD subset. However, CK levels and the muscular VAS score were lower in the ILD subset. These findings could reflect the high frequency of CADM in the ILD subset.

Table 2 Cytokine levels in PM/DM/CADM patients and HCs

	PM/DM/CADM ($n = 38$), median (IQR), pg/ml	HCs ($n = 15$), median (range), pg/ml
IL-1β	0 (0–0.5)**	0 (0–0)
IL-2	1.0 (0.4–1.8)***	0.2 (0–0.9)
IL-4	0.5 (0–3.0)**	0 (0–3.1)
IL-6	4.3 (1.0–7.3)***	0 (0–1.3)
IL-8	16.1 (11.8–26.7)***	1.7 (0.9–6.0)
IL-10	6.6 (1.6–13.8)***	0 (0–0)
IL-12	0.8 (0–2.8)	0 (0–13.6)
IL-13	0 (0–0)	0 (0–0)
IL-17	0.5 (0–1.3)	1.1 (0–6.9)
TNF-α	16.8 (10.6–29.3)***	2.0 (0.6–4.3)
IFN-α	12.2 (5.5–33.2)***	1.6 (0–4.7)
IFN-γ	1.6 (0.4–3.1)**	0.5 (0.9–1.6)
IP-10	5706 (1622–13195)***	67 (45–583)

Statistical analyses were performed using the Mann–Whitney U test to compare the PM/DM/CADM subset and HCs. $^{**}P < 0.01$ and $^{***}P < 0.001$. IQR: interquartile range; CADM: clinically amyopathic DM; HCs: healthy controls; IP-10: IFN-γ-inducible 10-kDa protein.

Analysis of cytokines that contribute to ILD in PM/DM/CADM

The levels of IL-4, IL-6, IL-8, IL-10, TNF-α and IP-10 were significantly higher in the ILD subset than the non-ILD subset (Table 4). To reveal the cytokines that contribute to ILD, multiple linear regression analysis was performed. The existence of ILD was the dependent variable. Independent variables included the above-described cytokines determined to be significant by univariate analysis. In addition, the multivariate analysis was adjusted with the muscular VAS and cutaneous VAS to reveal specific cytokines associated with pulmonary disease activity. TNF-α was the cytokine that was most significantly associated with ILD in PM/DM/CADM [$P = 0.0006$, odds ratio (OR) 1.4, CI 1.1, 2.2]. No other cytokines were significantly associated with ILD in multivariate analysis.

Comparison of cytokine profiles of the anti-ARS-ILD subset and anti-MDA5-ILD subset

To reveal the pathophysiological differences between anti-ARS-ILD and anti-MDA5-ILD, clinical characteristics and cytokine levels were compared between the two subsets. As shown in Table 5, in the anti-MDA5-ILD subset, the frequency of CADM complicated with RP-ILD was high and PM was not observed. The cutaneous VAS and pulmonary VAS scores were significantly higher in the anti-MDA5-ILD subset than in the anti-ARS-ILD subset, although the MITAX score and pulmonary function did not differ between the two subsets.

Regarding the cytokine levels, the IL-8 level was significantly higher in the anti-MDA5-ILD subset than the anti-ARS-ILD subset. Lower levels of IL-4 and higher levels of IL-10 and IFN-α were found in the anti-MDA5-ILD subset than in the anti-ARS-ILD subset, although these differences did not reach significance ($P < 0.10$). IL-6, TNF-α and IP-10 levels were high in both subsets and did not significantly differ between the two subsets.

Table 3 Correlations in each cytokine in PM/DM/CADM

	IL-1β	IL-2	IL-4	IL-6	IL-8	IL-10	IL-12	IL-13	IL-17	TNF-α	IFN-α	IFN-γ
IL-1β	–	–	–	–	–	–	–	–	–	–	–	–
IL-2	0.72***	–	–	–	–	–	–	–	–	–	–	–
IL-4	0.40*	0.43**	–	–	–	–	–	–	–	–	–	–
IL-6	0.55***	0.42**	0.23	–	–	–	–	–	–	–	–	–
IL-8	0.11	0.19	0.01	0.47**	–	–	–	–	–	–	–	–
IL-10	0.15	0.42**	0.09	0.39*	0.44**	–	–	–	–	–	–	–
IL-12	0.67***	0.75***	0.31	0.33*	0.17	0.37*	–	–	–	–	–	–
IL-13	0.39*	0.33*	0.27	0.22	0.08	0.15	0.33*	–	–	–	–	–
IL-17	0.04	0.28	−0.09	−0.13	0.32*	0.42**	0.42**	0.26	–	–	–	–
TNF-α	0.30	0.34*	0.43**	0.72***	0.41*	0.56***	0.16	0.15	−0.22	–	–	–
IFN-α	0.16	0.09	0.13	0.26	0.14	0.21	0.02	0.17	0.05	0.11	–	–
IFN-γ	0.31	0.42**	0.04	0.42**	0.28	0.58***	0.43**	0.31	0.37*	0.36*	0.21	–
IP-10	−0.02	0.13	0.37	0.42**	0.32*	0.60***	−0.06	0.007	−0.09	0.7	0.25	0.17

Statistical analyses were performed using Spearman's rank correlation coefficient. $^{*}P < 0.05$, $^{**}P < 0.01$ and $^{***}P < 0.001$.

To determine the cytokines that contributed to the pathophysiology of anti-MDA5 antibody ILD and anti-ARS antibody ILD, multiple linear regression analysis was performed. The existence of anti-MDA5 antibody positivity was the dependent variable. Independent variables included IL-4, IL-8, IL-10 and IFN-α levels, for which the *P*-value was <0.10 in the univariate analysis. IL-8 was the cytokine that was most significantly associated with anti-MDA5 antibody ILD ($P = 0.0006$, OR 1.5, CI 1.1, 3.0). In addition, IL-4 level was inversely associated with anti-MDA5 antibody ILD ($P = 0.01$, OR 0.8, CI 0.6, 0.98). Moreover, the ratio of serum IL-4 to IFN-γ, which may reflect a balance between T helper 1 (Th1) and 2 (Th2) cells, was lower in anti-MDA5 antibody ILD (median 0.16) than in anti-ARS antibody ILD (median 2.0), although this difference was not significant ($P = 0.07$).

TABLE 4 Comparison of the non-ILD subset and the ILD subset: clinical characteristics and cytokine profiles

	Non-ILD subset ($n = 17$)	ILD subset ($n = 21$)
Age, years	57 (40–64)	50 (37–56)
Female, *n* (%)	11 (65)	17 (81)
Duration, months	4 (2–13)	3 (2–6)
PM, DM, CADM, *n* (%)	9, 6, 2	3, 8, 10
CK, IU/l	1389 (417–4938)	285 (92–1573)*
VAS of disease activity, mm		
Constitutional VAS	14 (9–18)	50 (16–63)***
Muscular VAS	26 (10–42)	0 (0–38)
Cutaneous VAS	0 (0–46)	26 (12–42)
Skeletal VAS	0 (0–0)	0 (0–22)
Gastrointestinal VAS	0 (0–0)	0 (0–0)
Pulmonary VAS	0 (0–0)	37 (25–52)***
Cardiac VAS	0 (0–17)	0 (0–0)
MITAX	0.11 (0.05–0.16)	0.29 (0.16–0.38)***
Cytokines, pg/ml		
IL-1β	0 (0–2.1)	0 (0–0.5)
IL-2	0.2 (0.02–6.0)	1 (0.7–1.6)
IL-4	0 (0–1.0)	1.3 (0.5–4.1)**
IL-6	1 (0.4–5.4)	5.4 (2.1–10.7)*
IL-8	11.8 (9.2–21.9)	18.2 (14.2–29.4)*
IL-10	2.0 (0–9.5)	9.3 (5.2–20)**
IL-12	0.2 (0–20.5)	0.9 (0.2–2.5)
IL-13	0 (0–0)	0 (0–0)
IL-17	0.7 (0.3–1.3)	0.4 (0–1.2)
TNF-α	10.8 (8.6–15.5)	26.7 (17.6–36.7)***
IFN-α	13.6 (11.0–25.7)	8.4 (5.1–35.6)
IFN-γ	1.6 (0.4–3.1)	1.6 (0.5–3.8)
IP-10	2767 (853–9121)	9134 (3985–18 931)**

Values are given as median (interquartile range) unless stated otherwise. Statistical analyses were performed using the Mann–Whitney *U* test and Fisher's exact test to compare the non-ILD and ILD subsets. *$P < 0.05$, **$P < 0.01$ and ***$P < 0.001$. ILD: interstitial lung disease; CADM: clinically amyopathic DM; VAS: visual analogue scale; MITAX: myositis intention-to-treat activity index; IP-10: IFN-γ-inducible 10-kDa protein; CK: creatine kinase.

Prediction of fatal outcome due to ILD by serum cytokine levels

To predict a fatal outcome due to ILD, we estimated the cut-off levels of serum cytokines with all the ILD patients using a receiver operating characteristic (ROC) curve. The predictive cytokines included IL-8, IL-10 and IFN-α, which had high levels in anti-MDA5 antibody ILD. Fatal outcome due to ILD was found in four patients with anti-MDA5 antibody ILD, but none were found in patients with anti-ARS-ILD. The cut-off levels of serum cytokines (sensitivity, specificity) were as follows: IL-8, 29.7 pg/ml (100%, 94%); IL-10, 13.1 pg/ml (100%, 71%); IFN-α, 37.0 pg/ml (100%, 18%). Serum IL-8 was the most useful predictive cytokine for fatal outcome due to ILD.

In most patients without ILD, the cytokine levels were below the cut-off values, but a few patients had cytokine levels above the cut-off values. In the non-ILD subset with IL-8 levels above the cut-off value, all three patients had DM. All patients without ILD survived even if cytokine levels were above the cut-off values.

Comparison of cytokine profiles in active ILD status and improved ILD status

Clinical data and sera were also obtained after improvement of ILD in six patients (three with anti-ARS antibody and three with anti-MDA5 antibody). We compared disease activity and cytokine levels between the active ILD status time point and the improved ILD status time point in these six ILD patients.

As shown in Fig. 1, the MITAX and pulmonary disease activity VAS scores were significantly ($P < 0.05$) lower when the ILD status improved than when active, as expected. IL-6, TNF-α, IFN-α, IFN-γ and IP-10 levels were significantly ($P < 0.05$) decreased when the ILD status improved (Fig. 1). IL-1β, IL-2, IL-4 and IL-8 levels also decreased after improvement of ILD, although the differences were not significant.

Discussion

We have identified the cytokine profiles associated with PM, DM and CADM. IL-6, IL-8, IL-10, TNF-α and IP-10 levels were associated with the global disease activity of PM/DM/CADM in the present study. These results were consistent with those of previous studies [19, 20]. Serum biomarkers could be affected by the activity of several diseases, including dermatitis, myositis and ILD in PM/DM/CADM. The present study demonstrated that TNF-α was the most significant cytokine in ILD with PM/DM/CADM. In idiopathic pulmonary fibrosis (IPF), activated macrophages and TNF-α play a crucial role in pulmonary inflammation and/or fibrosis [21–23]. We speculate that TNF-α produced by activated macrophages and mononuclear cells could be associated with the development of ILD as well as myositis and dermatitis with PM/DM/CADM.

In general, activated macrophages are classified into three subsets: classically activated macrophages, wound-healing macrophages and regulatory macrophages [24]. Classically activated macrophages produce pro-inflammatory cytokines such as IL-1 and IL-6. IFN-γ produced by Th1 cells or natural killer cells, along with TNF-α from antigen-presenting cells, can stimulate classically activated macrophages. In contrast, wound-healing macrophages play a role in the release of pro-fibrotic mediators and in the deposition of collagen. IL-4 produced by Th2 cells or granulocytes can promote the activation of wound-healing macrophages. IL-4 is the most powerful inducer of wound-healing macrophages in IPF patients [25]. The imbalance between classically activated macrophages and wound-healing macrophages might cause the differences in pathophysiology between RP-ILD and chronic ILD in PM/DM/CADM.

This study also revealed differences in the cytokine profiles of anti-ARS-ILD and anti-MDA5-ILD. In patients with these antibody types, it has been reported in previously that clinical manifestations, response to therapy and prognosis of ILD vary in PM and DM [4]. Anti-MDA5-ILD is more intractable and life threatening than anti-ARS-ILD, especially in East Asia. Until now, the details of these differences in pathophysiology have remained unknown. We found that IL-4 levels were low in anti-MDA5-ILD patients and HCs, whereas they were higher in anti-ARS-ILD patients. The ratio of serum IL-4 to IFN-γ was also lower in anti-MDA5 antibody ILD than in anti-ARS antibody ILD. In anti-MDA5-ILD, the cytokine balance was skewed more dominantly to a Th1 profile than in anti-ARS-ILD. The balance between Th1 and Th2 cytokines may contribute to the differences in activated macrophage type, the severity of pulmonary inflammation and the response to treatment in anti-ARS-ILD and the anti-MDA5-ILD.

However, IL-8 levels were higher in anti-MDA5-ILD than anti-ARS-ILD. As the present study indicates, serum IL-8 is a useful predictor for fatal outcome due to ILD. The IL-8 levels in bronchoalveolar lavage fluid correlated with the severity of pneumocystis pneumonia [26]. In addition, plasma IL-8 levels were associated with the severity of acute lung injury (ALI)/ARDS [27, 28]. IL-8-related

Table 5 Comparison of the anti-ARS-ILD subset and the anti-MDA5-ILD subset: clinical characteristics and cytokine profiles

	Anti-ARS-ILD subset ($n = 11$)	Anti-MDA-5-ILD subset ($n = 10$)
Age, years	51 (44-56)	49 (25-58)
Female, *n* (%)	10 (90)	7 (70)
Duration, months	3 (2-6)	3 (3-6)
PM, DM, CADM, *n*	3, 6, 2	0, 2, 8
RP-ILD, *n* (%)	2 (18)	8 (80)***
CK, IU/l	1443 (285-2170)	97 (50-228)***
VAS of disease activity, mm		
Muscular VAS	35 (10-42)	0 (0-11)*
Constitutional VAS	39 (15-64)	50 (17-61)
Cutaneous VAS	13 (0-33)	42 (20-44)**
Skeletal VAS	0 (0-24)	0 (0-22)
Gastrointestinal VAS	0 (0-0)	0 (0-0)
Pulmonary VAS	27 (20-48)	47 (34-74)**
Cardiac VAS	0 (0-0)	0 (0-0)
MITAX	0.25 (0.11-0.38)	0.30 (0.21-0.38)
Pulmonary function		
P/F ratio, torr	373 (350-426) ($n = 10$)	379 (212-450) ($n = 8$)
A-aDO_2, mmHg	16 (5-26) ($n = 10$)	21 (3-33) ($n = 8$)
%VC, %	71 (52-93) ($n = 8$)	87 (71-104) ($n = 7$)
Cytokine, pg/ml		
IL-4	3.2 (1.1-9.2)	0.7 (0-1.8)*
IL-6	5.4 (1.0-10.6)	5.7 (3.2-16.8)
IL-8	14.4 (12.3-24.5)	26.0 (17.8-39.1)***
IL-10	6.8 (3.9-14.2)	13.4 (8.5-40.8)*
TNF-α	29.8 (19.6-41.7)	23.5 (15.6-31.1)
INF-α	5.6 (1.2-9.7)	33.7 (6.4-51.1)*
INF-γ	1.4 (0.4-2.8)	2.2 (0.5-6.1)
IP-10	8024 (2979-19 199)	10 960 (4369-19 003)

Values are given as median (interquartile range) unless stated otherwise. Statistical analyses were performed using the Mann–Whitney *U* test and Fisher's exact test. *$P < 0.10$, **$P < 0.05$ and ***$P < 0.01$. ARS: aminoacyl-tRNA synthetase; ILD: interstitial lung disease; MDA5: melanoma differentiation-associated gene 5; RP-ILD: rapidly progressive ILD; MITAX: myositis intention-to-treat activity index; P/F ratio: arterial oxygen tension (PaO_2)/fractional inspired oxygen (F_iO_2) ratio; A-aDO_2: alveolar-arterial oxygen difference; %VC: vital capacity percentage; IP-10: IFN-γ-inducible 10-kDa protein; CK: creatine kinase.

neutrophil elastase may play a role in the pathogenesis of ALI/ARDS. Alveolar macrophages activated by some antigens, microbes and autoimmune stimuli are induced to produce IL-8, which stimulates neutrophils and thereby induces fibrosis in the lungs [29]. Diffuse alveolar damage has been found in both ALI/ARDS and anti-MDA5-ILD. The common pathophysiology could result from the activated alveolar macrophages and neutrophils in these two diseases. IL-8 could be a key cytokine and a target for therapy in anti-MDA5-ILD.

IFN-α and IFN-α-inducible genes are associated with the whole disease status of PM/DM [30, 31]. Serum IFN-α levels were also high in anti-MDA5-ILD in the present study. Previous studies have reported that IFN-α may be more closely and strongly associated with pulmonary disease status in anti-MDA5-ILD [12]. The MDA5 protein plays a role in the innate immune system. MDA5 initially recognizes picorna viruses, such as the Coxsackie virus, and induces antiviral responses by inducing the production of type I IFNs and TNF-α [32]. Hyperferritinaemia is revealed not only in macrophage activation syndrome (MAS), but also in RP-ILD with anti-MDA5 antibodies [10, 11, 33]. The pathophysiology of MAS involves the lack of regulation of T lymphocytes and excessive production of cytokines such as TNF-α, IL-1β IL-6 and IL-18, resulting in the activation of macrophages. The activated promotion of IFN-α and TNF-α via MDA5 protein may cause stimulation of Th1 cells and macrophages as well as the development of a cytokine storm in the lungs in patients with anti-MDA5-ILD.

There are several limitations to this study. First, this study was retrospectively conducted. The MITAX and MYOACT scores were retrospectively estimated. Secondly, patients with PM and DM were combined and classified into the non-ILD subset. In general, the pathophysiology of PM is distinct from that of DM, although some cytokines, including IL-6, TNF-α and IP-10, are commonly associated with the inflammation of muscle tissue in both PM and DM. Thirdly, PM/DM-ILD patients without either anti-MDA5 or anti-ARS were not enrolled in this study. Some results might be not valid in the whole aspect of PM/DM-ILD. Finally, some patients were being treated with intermediate or high-dose prednisolone at the time of serum collection. These medications could influence the measurement of cytokine levels, although almost all patients were being treated with low-dose prednisolone (0.1–0.2 mg/kg/day) or with symptomatic therapy when serum was collected.

In conclusion, IL-6, IL-8, IL-10, TNF-α and IP-10 are associated with global disease activity in PM, DM and CADM. These cytokine levels were high, especially in ILD with PM/DM. Serum IL-8 levels and the balance between IL-4 and IFN-γ may contribute to the differences in pathophysiology between chronic ILD (anti-ARS-ILD) and RP-ILD (anti-MDA5-ILD).

Fig. 1 Comparison of disease activity and cytokine levels in patients with active ILD status and improved ILD status

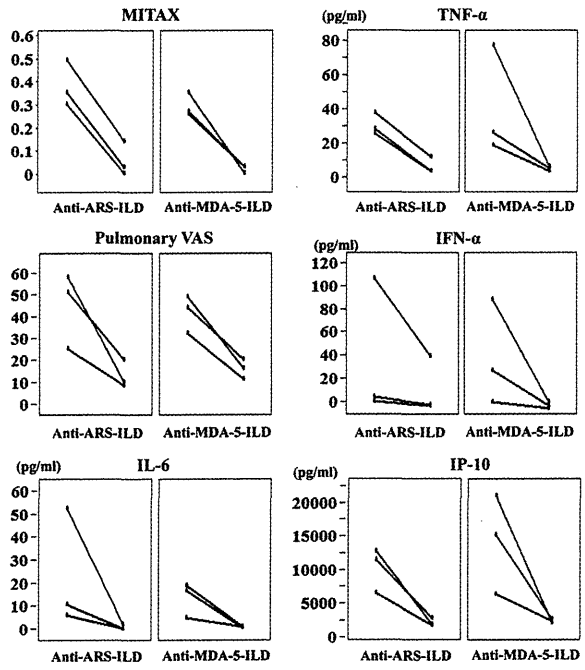

Statistical analyses were performed using the Wilcoxon signed-rank test to compare the active ILD status group and the improved ILD status group. MITAX, pulmonary VAS, IL-6, TNF-α, IFN-α and IP-10 levels were significantly ($P < 0.05$) decreased when the ILD status improved. MITAX: myositis intention-to-treat activity index; VAS: visual analogue scale; IP-10: IFN-γ-inducible 10-kDa protein.

Rheumatology key messages

- IL-6, IL-8 and TNF-α are associated with disease activity in PM/DM.
- Serum IL-8 is a useful predictor for fatal outcomes due to ILD with PM/DM.

Acknowledgements

All authors contributed to the design of the study, the analysis of data and the writing of the manuscript. Each author reviewed the final version of the manuscript and approved it for publication.

Funding: This study was supported in part by research grants from Japan's Ministry of Health, Labour and Welfare.

Disclosure statement: The authors have declared no conflicts of interest.

References

1 Callen J. Dermatomyositis. Lancet 2000;355:53–7.

2 Ernste FC, Reed AM. Idiopathic inflammatory myopathies: current trends in pathogenesis, clinical features, and

up-to-date treatment recommendations. Mayo Clin Proc 2013;88:83–105.

3 Miller FW. New approaches to the assessment and treatment of the idiopathic inflammatory myopathies. Ann Rheum Dis 2012;71(Suppl 2):i82–5.

4 Mimori T, Nakashima R, Hosono Y. Interstitial lung disease in myositis: clinical subsets, biomarkers, and treatment. Curr Rheumatol Rep 2012;14:264–74.

5 Marie I. Morbidity and mortality in adult polymyositis and dermatomyositis. Curr Rheumatol Rep 2012;14:275–85.

6 De Paepe B, Creus KK, De Bleecker JL. Role of cytokines and chemokines in idiopathic inflammatory myopathies. Curr Opin Rheumatol 2009;21:610–6.

7 Richards TJ, Eggebeen A, Gibson K *et al.* Characterization and peripheral blood biomarker assessment of anti-Jo-1 antibody-positive interstitial lung disease. Arthritis Rheum 2009;60:2183–92.

8 Labirua A, Lundberg IE. Interstitial lung disease and idiopathic inflammatory myopathies: progress and pitfalls. Curr Opin Rheumatol 2010;22:633–8.

9 Sato S, Hoshino K, Satoh T *et al.* RNA helicase encoded by melanoma differentiation-associated gene 5 is a major autoantigen in patients with clinically amyopathic dermatomyositis: association with rapidly progressive interstitial lung disease. Arthritis Rheum 2009;60:2193–200.

10 Nakashima R, Imura Y, Kobayashi S *et al.* The RIG-I-like receptor IFIH1/MDA5 is a dermatomyositis-specific autoantigen identified by the anti-CADM-140 antibody. Rheumatology 2010;49:433–40.

11 Gono T, Kawaguchi Y, Satoh T *et al.* Clinical manifestation and prognostic factor in anti-melanoma differentiation-associated gene 5 antibody-associated interstitial lung disease as a complication of dermatomyositis. Rheumatology 2010;49:1713–9.

12 Sun WC, Sun YC, Lin H, Yan B, Shi GX. Dysregulation of the type I interferon system in adult-onset clinically amyopathic dermatomyositis has a potential contribution to the development of interstitial lung disease. Br J Dermatol 2012;167:1236–44.

13 Bohan A, Peter J. Polymyositis and dermatomyositis (first of two parts). N Engl J Med 1975;292:344–7.

14 Sontheimer R. Would a new name hasten the acceptance of amyopathic dermatomyositis (dermatomyositis siné myositis) as a distinctive subset within the idiopathic inflammatory dermatomyopathies spectrum of clinical illness? J Am Acad Dermatol 2002;46:626–36.

15 American Thoracic Society and European Respiratory Society. American Thoracic Society/European Respiratory Society International Multidisciplinary Consensus Classification of the Idiopathic Interstitial Pneumonias. This joint statement of the American Thoracic Society (ATS), and the European Respiratory Society (ERS) was adopted by the ATS board of directors, June 2001 and by the ERS Executive Committee, June 2001. Am J Respir Crit Care Med 2002;165:277–304.

16 Bonaccorsi A, Cancellieri A, Chilosi M *et al.* Acute interstitial pneumonia: report of a series. Eur Respir J 2003;21:187–91.

17 Miller FW, Rider LG, Chung YL *et al.* Proposed preliminary core set measures for disease outcome assessment in adult and juvenile idiopathic inflammatory myopathies. Rheumatology 2001;40:1262–73.

18 IMACS website. Disease activity core set measures. http://www.niehs.nih.gov/research/resources/collab/imacs/diseaseactivity/index.cfm (4 June 2014, date last accessed).

19 Bilgic H, Ytterberg SR, Amin S *et al.* Interleukin-6 and type I interferon-regulated genes and chemokines mark disease activity in dermatomyositis. Arthritis Rheum 2009;60:3436–46.

20 Reed AM, Peterson E, Bilgic H *et al.* Changes in novel biomarkers of disease activity in juvenile and adult dermatomyositis are sensitive biomarkers of disease course. Arthritis Rheum 2012;64:4078–86.

21 Miyazaki Y, Araki K, Vesin C *et al.* Expression of a tumor necrosis factor-alpha transgene in murine lung causes lymphocytic and fibrosing alveolitis. A mouse model of progressive pulmonary fibrosis. J Clin Invest 1995;96:250–9.

22 Freeburn RW, Armstrong L, Millar AB. Cultured alveolar macrophages from patients with idiopathic pulmonary fibrosis (IPF) show dysregulation of lipopolysaccharide-induced tumor necrosis factor-alpha (TNF-alpha) and interleukin-10 (IL-10) inductions. Eur Cytokine Netw 2005;16:5–16.

23 Bargagli E, Prasse A, Olivieri C, Muller-Quernheim J, Rottoli P. Macrophage-derived biomarkers of idiopathic pulmonary fibrosis. Pulm Med 2011;2011:717130.

24 Mosser DM, Edwards JP. Exploring the full spectrum of macrophage activation. Nat Rev Immunol 2008;8:958–69.

25 Pechkovsky DV, Prasse A, Kollert F *et al.* Alternatively activated alveolar macrophages in pulmonary fibrosis-mediator production and intracellular signal transduction. Clin Immunol 2010;137:89–101.

26 Benfield TL, Vestbo J, Junge J *et al.* Prognostic value of interleukin-8 in AIDS-associated Pneumocystis carinii pneumonia. Am J Respir Crit Care Med 1995;151:1058–62.

27 Agrawal A, Zhuo H, Brady S *et al.* Pathogenetic and predictive value of biomarkers in patients with ALI and lower severity of illness: results from two clinical trials. Am J Physiol Lung Cell Mol Physiol 2012;303:L634–9.

28 Groeneveld AB, Raijmakers PG, Hack CE, Thijs LG. Interleukin 8-related neutrophil elastase and the severity of the adult respiratory distress syndrome. Cytokine 1995;7:746–52.

29 Ward P, Hunninghake G. Lung inflammation and fibrosis. Am J Respir Crit Care Med 1998;157(4 Pt 2):S123–9.

30 Greenberg SA, Pinkus JL, Pinkus GS *et al.* Interferon-alpha/beta-mediated innate immune mechanisms in dermatomyositis. Ann Neurol 2005;57:664–78.

31 Walsh RJ, Kong SW, Yao Y *et al.* Type I interferon-inducible gene expression in blood is present and reflects disease activity in dermatomyositis and polymyositis. Arthritis Rheum 2007;56:3784–92.

32 Takeuchi O, Akira S. MDA5/RIG-I and virus recognition. Curr Opin Immunol 2008;20:17–22.

33 Tristano A. Macrophage activation syndrome: a frequent but under-diagnosed complication associated with rheumatic diseases. Med Sci Monit 2008;14:RA27–36.

RHEUMATOLOGY

Rheumatology 2014;53:2204–2208
doi:10.1093/rheumatology/keu259
Advance Access publication 1 July 2014

Concise report

Calcinosis in juvenile dermatomyositis is influenced by both anti-NXP2 autoantibody status and age at disease onset

Sarah L. Tansley[1], Zoe E. Betteridge[2], Gavin Shaddick[3], Harsha Gunawardena[4], Katie Arnold[5,6], Lucy R. Wedderburn[5,6] and Neil J. McHugh[1], on behalf of the Juvenile Dermatomyositis Research Group

Abstract

Objective. Calcinosis is a major cause of morbidity in JDM and has previously been linked to anti-NXP2 autoantibodies, younger age at disease onset and more persistent disease activity. This study aimed to investigate the clinical associations of anti-NXP2 autoantibodies in patients with JDM stratified by age at disease onset.

Methods. A total of 285 patients with samples and clinical data were recruited via the UK Juvenile Dermatomyositis Cohort and Biomarker Study. The presence of anti-NXP2 was determined by both immunoprecipitation and ELISA. Logistic regression analysis was performed to assess the age-dependent relationship between anti-NXP2 and the development of calcinosis and disease activity measures.

Results. We identified anti-NXP2 autoantibodies in 56 patients (20%). While in all patients younger age at disease onset was associated with an increased risk of calcinosis and this relationship was nearly linear, anti-NXP2 autoantibodies substantially increased the risk of calcinosis across all ages ($P = 0.025$) and were detectable prior to calcinosis development. Children with anti-NXP2 autoantibodies had a greater degree of weakness (median lowest ever Childhood Myositis Assessment Score 29.6 *vs* 42) and were less likely to be in remission at 2 years post-diagnosis. No difference in disease activity was seen 4 years post-diagnosis.

Conclusion. Children diagnosed at a young age have a high risk of calcinosis regardless of autoantibody status. However, the presence of anti-NXP2 autoantibodies substantially increases the risk of calcinosis across all ages and is associated with disease severity.

Key words: juvenile dermatomyositis, autoantibody, calcinosis, age.

Introduction

Our group has previously demonstrated that antibodies to a 140 kDa protein detected by protein immunoprecipitation (known as anti-p140 or P140) in JDM were strongly associated with the development of calcinosis, a major cause of morbidity [1]. The presence of autoantibodies to a 142 kDa antigen (anti-MJ) in JDM has also been shown by others to be associated with a severe disease course, worse functional status and persistent disease activity [2]. It is now clear that the target of these autoantibodies is a 140 kDa protein, NXP2 (molecular weight 140 kDa). Anti-NXP2 autoantibodies are common in JDM and identifiable in 13–23% of patients [1, 2].

JDM is a heterogeneous disease and autoantibodies are potentially useful biomarkers to divide patients into homogeneous subgroups and inform on prognosis. Anti-NXP2 autoantibodies are of particular interest, given their

[1]Royal National Hospital for Rheumatic Diseases NHS Foundation Trust, [2]Department of Pharmacy and Pharmacology, University of Bath, [3]Department of Mathematical Sciences, University of Bath, Bath, [4]Department of Rheumatology, Southmead Hospital, North Bristol NHS Trust, Bristol, [5]Rheumatology Unit, University College London Institute of Child Health and [6]Arthritis Research UK Centre for Adolescent Rheumatology at University College London, University College London Hospital and Great Ormond Street Hospital, London, UK.

Submitted 18 November 2013; revised version accepted 2 May 2014.

Correspondence to: Neil J. McHugh, Royal National Hospital for Rheumatic Diseases NHS Foundation Trust, Upper Borough Walls, Bath BA1 1RL, UK. E-mail: Neil.McHugh@rnhrd.nhs.uk

PLOS | ONE

Association between a *C8orf13–BLK* Polymorphism and Polymyositis/Dermatomyositis in the Japanese Population: An Additive Effect with *STAT4* on Disease Susceptibility

Tomoko Sugiura[1], Yasushi Kawaguchi[1]*, Kanako Goto[2], Yukiko Hayashi[2], Takahisa Gono[1], Takefumi Furuya[1], Ichizo Nishino[2], Hisashi Yamanaka[1]

1 Institute of Rheumatology, Tokyo Women's Medical University, Tokyo, Japan, **2** Department of Neuromuscular Research, National Institute of Neuroscience, and Department of Clinical Development, Translational Medical Center, National Center of Neurology and Psychiatry, Tokyo, Japan

Abstract

Background: Accumulating evidence has shown that several non-HLA genes are involved in the susceptibility to polymyositis/dermatomyositis. This study aimed to investigate the involvement of *C8orf13–BLK*, one of the strongest candidate genes for autoimmune diseases, in susceptibility to polymyositis/dermatomyositis in the Japanese population. A possible gene–gene interaction between *C8orf13–BLK* and *STAT4*, which we recently showed to be associated with Japanese polymyositis/dermatomyositis, was also analyzed.

Methods: A single-nucleotide polymorphism in *C8orf13–BLK* (dbSNP ID: rs13277113) was investigated in the Japanese population using a TaqMan assay in 283 polymyositis patients, 194 dermatomyositis patients, and 656 control subjects.

Results: The *C8orf13–BLK* rs13277113A allele was associated with overall polymyositis/dermatomyositis ($P<0.001$, odds ratio [OR] 1.44, 95% confidence interval [CI] 1.19–1.73), as well as polymyositis ($P=0.011$, OR 1.32, 95% CI 1.06–1.64) and dermatomyositis ($P<0.001$, OR 1.64, 95% CI 1.26–2.12). No association was observed between the *C8orf13–BLK* rs13277113A allele and either interstitial lung disease or anti-Jo-1 antibody positivity. The *C8orf13–BLK* rs13277113 A and *STAT4* rs7574865 T alleles had an additive effect on polymyositis/dermatomyositis susceptibility. The strongest association was observed in dermatomyositis, with an OR of 3.07 (95% CI; 1.57–6.02) for the carriers of four risk alleles at the two SNP sites, namely, rs1327713 and rs7574865.

Conclusions: This study established *C8orf13–BLK* as a new genetic susceptibility factor for polymyositis/dermatomyositis. Both *C8orf13–BLK* and *STAT4* exert additive effects on disease susceptibility. These observations suggested that *C8orf13–BLK*, in combination with *STAT4*, plays a pivotal role in creating genetic susceptibility to polymyositis/dermatomyositis in Japanese individuals.

Citation: Sugiura T, Kawaguchi Y, Goto K, Hayashi Y, Gono T, et al. (2014) Association between a *C8orf13–BLK* Polymorphism and Polymyositis/Dermatomyositis in the Japanese Population: An Additive Effect with *STAT4* on Disease Susceptibility. PLoS ONE 9(3): e90019. doi:10.1371/journal.pone.0090019

Editor: Ralf Andreas Linker, Friedrich-Alexander University Erlangen, Germany

Received October 10, 2013; **Accepted** January 29, 2014; **Published** March 14, 2014

Funding: This study was supported by autoimmune disease research grants from the Ministry of Health, Labor, and Welfare, Japan and was partly supported by an Intramural Research Grant (23-4, 23-5) for Neurological and Psychiatric Disorders from the National Center of Neurology and Psychiatry. The funders had no role in study design, data collection and analysis, decision to publish, or preparation of the manuscript.

Competing Interests: The authors have declared that no competing interests exist.

* E-mail: y-kawa@ior.twmu.ac.jp

Introduction

Polymyositis and dermatomyositis are rare connective tissue diseases, with unknown etiologies, which belong to the idiopathic inflammatory myopathies (IIMs). The typical clinical features are symmetrical and include proximal weakness of skeletal muscles and infiltrating mononuclear cells seen in muscle biopsies, and may be accompanied by skin rash. The diagnosis of IIMs in 29% of patients is accompanied by other connective tissue diseases (CTDs), such as systemic sclerosis (SSc), systemic lupus erythematosus (SLE), and rheumatoid arthritis (RA) [1], suggesting that IIMs are associated with general autoimmunity.

Although most immunogenetic IIM investigators have focused on the polymorphic genes of the major histocompatibility complex (human leucocyte antigen [HLA]) [2], new genetic markers have been identified outside the HLA region. For example, the R620W polymorphism of the protein tyrosine phosphatase N22 gene (*PTPN22*), one of the most well-documented risk genes for several autoimmune diseases specific for Caucasians [3], was found to be associated with IIMs in British Caucasian patients [4]. Moreover, we have recently shown that a polymorphism (rs7574865) in the signal transducer and activator of transcription 4 gene (*STAT4*) is associated with adult-onset polymyositis and dermatomyositis in a Japanese population [5]. After being identified as a risk gene for

SLE and RA [6], *STAT4* was also associated with susceptibility to a number of other autoimmune diseases, irrespective of ethnicity [7]. These observations strongly suggested that IIMs share an 'autoimmune-prone' genetic background with other autoimmune diseases.

BLK encodes a B lymphoid-specific tyrosine kinase of the Src family, which is involved in B cell receptor-mediated signaling and B cell development [8]. The risk allele (A) of rs13277113 (rs13277113A) within the *C8orf13–BLK* region of chromosome 8p23–p22 was originally identified in SLE patients by a genome-wide association study (GWAS) [9]. This polymorphism is associated with low levels of *BLK* mRNA and high levels of *C8orf13* mRNA, which encodes a ubiquitously expressed gene of unknown function [9]. An association between *C8orf13–BLK* polymorphisms and SLE was first identified in North Americans of European descent and in Swedish populations [9], and was later replicated in both European [10] and Asian populations [11]. Subsequently, other autoimmune diseases, such as SSc [12,13] and RA [14], were shown to be associated with polymorphisms in *C8orf13–BLK*.

The contribution of *C8orf13–BLK* appears to be prominent in Asian populations, in which the risk allele rs13277113A is the major allele. Indeed, the allele frequency of rs13277113A is approximately 0.65 in the Japanese population [11,12], compared with approximately 0.25 in North American and European populations [9,13,14]. In Japanese SLE patients, a positive association between disease susceptibility and this polymorphism in *C8orf13–BLK* was confirmed with an OR of 2.44 [11], whereas the OR was 1.39 in Caucasian populations [9]. A similar increase in OR was observed in Japanese SSc patients compared with Caucasian patients [12,13].

Therefore, genetic variants of *C8orf13–BLK* could strongly contribute to lowering the disease threshold for autoimmune diseases, and particularly in Asian populations. In this study, we investigated whether *C8orf13–BLK* variants contribute to disease susceptibility in Japanese polymyositis/dermatomyositis patients and assessed any potential additive effects between *C8orf13–BLK* and *STAT4* in the susceptibility to polymyositis/dermatomyositis.

Patients and Methods

Subjects

This study was reviewed and approved by the research ethics committees of both the Tokyo Women's Medical University (TWMU) and National Center of Neurology and Psychiatry (NCNP) and complied with the Helsinki Declaration.

We enrolled patients who had probable or definite myositis based on the criteria of Bohan and Peter [15] and who were 18 years of age or older at disease onset. For our study, dermatomyositis patients included those with clinically defined amyopathic dermatomyositis who fulfilled the traditional criteria of Sontheimer [16]. Patients with myositis overlapping with other CTDs, such as RA, SLE, and SSc, were excluded from the study because these CTDs have previously been associated with *C8orf13–BLK* variants [9–14]. Patients with inherited, metabolic, or infectious myopathies and with inclusion body myositis were also excluded. All patients underwent a muscle biopsy.

The polymyositis/dermatomyositis patients were recruited from two different institutions: 138 (46 polymyositis and 92 dermatomyositis patients) were recruited from the Institute of Rheumatology, TWMU (Tokyo, Japan), and 339 (237 polymyositis and 102 dermatomyositis patients) were recruited from the National Institute of Neuroscience, NCNP (Kodaira City, Tokyo, Japan). In total, 477 patients with adult-onset polymyositis/dermatomyositis (69.8% female) were retrospectively investigated, including 283 polymyositis patients (68.3% female) and 194 dermatomyositis patients (71.1% female). The mean ages of the polymyositis and dermatomyositis patients were 51.4±15.8 and 52.3±16.5 y, respectively. None of the patients were genetically related.

As controls, we enrolled healthy unrelated individuals from the Tokyo area (n = 656; 57.1% female; mean age = 38.6±11.9 years). All patients and control subjects were Japanese individuals, and they were living in the central part of mainland Japan (Honshu).

For a sub-analysis of association between the *C8orf13–BLK* rs13277113 polymorphism and the presence or absence of interstitial lung disease (ILD) or serological status, 138 polymyositis/dermatomyositis patients recruited from TWMU were evaluated. The presence of ILD was confirmed or excluded by computed tomography (CT), high-resolution CT, if available, and spirometry. For serological analysis, the only association between the possession of the anti-Jo-1 antibody and *C8orf13–BLK* rs13277113A was analyzed, because not all patients were screened for other myositis-specific autoantibodies (MSAs).

Genotyping

To date, rs13277113 within *C8orf13–BLK* and the related single nucleotide polymorphism (SNP) have shown the strongest association with several autoimmune diseases [9–14]. Given this background, and our previous findings, the *C8orf13–BLK* rs13277113 and *STAT4* rs7574865 genotypes were determined using a TaqMan fluorogenic 5′-nuclease assay, according to the manufacturer's instructions (Applied Biosystems, Carlsbad, CA, USA). End-point fluorescence was measured with an ABI Prism 7900 HT Sequence Detection System (Applied Biosystems). In the disease subgroups and the control group, none of the SNPs deviated from Hardy–Weinberg equilibrium.

Statistical analysis

Association analyses were performed using chi-square tests for 2×2 contingency tables. Bonferroni's correction was applied for association analyses between the *C8orf13–BLK* polymorphism and the three clinical subsets (polymyositis, dermatomyositis, and polymyositis/dermatomyositis patients versus controls) and was expressed as *Pcorr*. The odds ratios (ORs) and 95% confidence intervals (95% CIs) were also determined. A logistic regression model was applied to assess gene–gene interactions between *C8orf13–BLK* rs13277113 and *STAT4* rs7574865 by using SPSS (Statistical Package for the Social Sciences) software version 19.0 (SPSS, Chicago, IL, USA) and to determine the additive effects of these two SNPs. Regression analysis accounted for the combination of the genotypes from both loci; thus, each individual had 0–4 risk alleles when considering both SNP sites. The ORs were computed using a logistic regression model, with individuals carrying 0 or 1 risk allele as a reference. The difference in the *C8orf13–BLK* and *STAT4* risk allele counts between the patients and control subjects was analyzed using Fisher's exact test. Statistical analyses were conducted using SPSS version 19.0 (SPSS).

Power calculations were performed using the Quanto software (http://hydra.usc.edu/gxe/) for case–control analysis, using a significance level of 0.05. Power was calculated to be 0.78 using the ORs previously reported in Japanese collagen disease [12] and the present study, as well as the sample size and risk allele frequency in the present study. Under the same parameter settings, 503 patients would be needed to demonstrate an OR of 1.44, at an alpha of 0.05, with power of 0.8. Similarly, to gain power of 0.9, 665 patients would be needed.